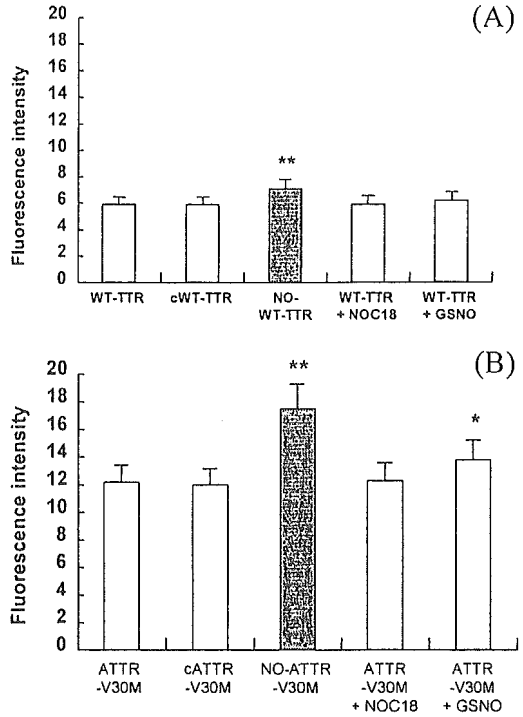

FIGURE 5: Amyloid formation of TTRs in the presence of exogenous NO. Samples of 15 μM unmodified or *S*-nitrosylated WT TTR and ATTR V30M were incubated in 50 mM sodium acetate and 100 mM KCl at pH 3.0 in the presence or absence of 50 μM NOC18 and GSNO. Amyloidogenicity was examined under the same conditions that are described in the legend of Figure 4: (A) WT TTR and (B) ATTR V30M. cTTRs are TTRs that underwent the same procedure as the *S*-nitrosylated TTRs but without IAN. Two asterisks indicate that $p < 0.01$, for unmodified TTRs vs *S*-nitrosylated TTRs at pH 3.0. One asterisk indicates that $p < 0.05$, for unmodified ATTR V30M vs TTR incubated with GSNO.

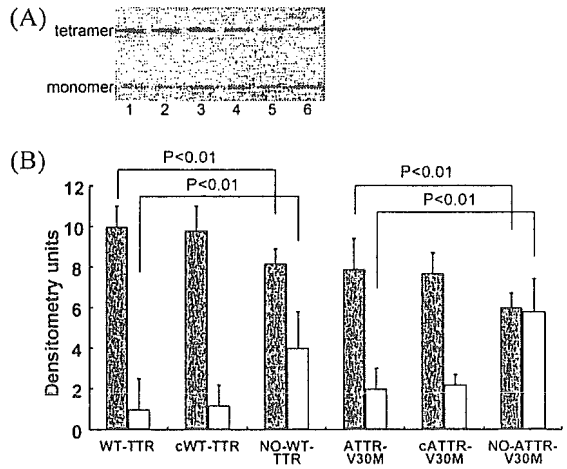

FIGURE 6: Effect of S-nitrosylation on the stability of the tetrameric forms of TTRs. Samples of 15 μM unmodified or *S*-nitrosylated WT TTR and ATTR V30M were incubated at 37 °C for 5 days in acetate buffer (pH 3.0). (A) Samples were analyzed via nonboiled (nonreducing) SDS−PAGE as described in the text: lane 1, WT TTR; lane 2, WT cTTR; lane 3, NO-bound WT TTR; lane 4, ATTR V30M; lane 5, cATTR V30M; and lane 6, NO-bound ATTR V30M. (B) Intensities of the bands were evaluated by densitometric analysis (ATTO densito, ATTO, Tokyo, Japan): (white columns) TTR monomers and (gray columns) TTR tetramers.

induces transnitrosylation, which occurs even at acidic pH, and in those solutions, TTRs may undergo S-nitrosylation (*19*). These results suggest that NO dissociated from TTR may not directly participate in amyloid fibril formation.

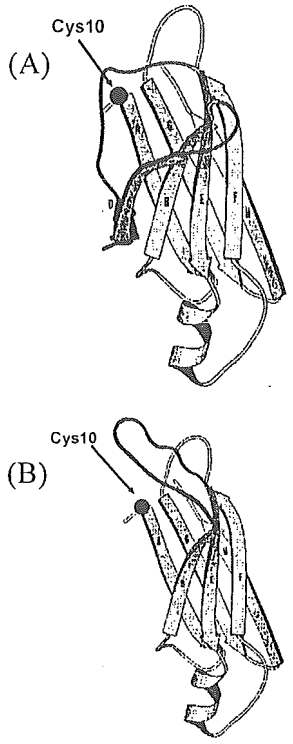

FIGURE 7: Conformation of WT TTR and ATTR V30M. A change in TTR structure caused by an amino acid substitution may induce amyloid formation by facilitating dissociation of TTR tetramers to monomers, which leads to amyloid fibril formation via misfolding C−D strands of the TTR molecule. S-Nitrosylation in TTRs may be one of the factors facilitating dissociation of TTR tetramers to monomers.

It is widely accepted that a change in TTR structure caused by an amino acid mutation may induce amyloid formation by facilitating dissociation of TTR tetramers to monomers (*42*) (Figure 7). To elucidate the mechanism of the increased amyloidogenicity in *S*-nitrosylated TTRs, we used nonboiled (nonreducing) SDS−PAGE to examine the ratio of tetramers to monomers for *S*-nitrosylated WT TTR and ATTR V30M. As Figure 6 shows, *S*-nitrosylated TTRs had higher ratios of monomeric to tetrameric forms than did unmodified TTRs, and the proportion of the monomeric form of *S*-nitrosylated ATTR V30M was greater than that of *S*-nitrosylated WT TTR. These results indicate that the increase in the extent of monomer formation occurs depending on S-nitrosylation of TTRs. This analysis and other conformational studies thus suggest that S-nitrosylation of TTRs induced a change in TTR structure, leading to reduced tetrameric stability and enhancing the amyloidogenicity of TTRs.

Unmodified Cys residues of circulating plasma proteins such as albumin and α_1-protease inhibitor undergo S-nitrosylation, and these *S*-nitrosylated proteins protect against tissue injury (*43*). However, as Figure 5 demonstrates, *S*-nitrosylated TTR would function as a harmful protein for amyloid fibril formation, whereas *S*-nitrosylated TTR in the bloodstream may work as a beneficial molecule for tissue injury, like *S*-nitrosylated albumin and α_1-protease inhibitor (*18*, *44*, *45*). Further study is needed.

In all types of TTR-related FAP, perivascular sites are known to show the greatest level of amyloid deposition, although the reason for this finding has not been well explained. These lesions are locations of NO reactions, where endothelial cells of vessels and smooth muscles generate NO.

In fact, nitrotyrosine antibody exhibited perivascular immunoreactivity at sites of abundant amyloid deposition in transgenic mice with ATTR V30M (*26*).

In conclusion, ATTR V30M was more prone to undergoing S-nitrosylation than WT TTR. *S*-Nitrosylated TTRs, especially ATTR V30M, induced formation of amyloid fibrils after a change in conformation. FAP, whose precursor protein is primarily ATTR V30M, usually starts to produce clinical manifestations when patients are ~35−45 years old; SSA, whose precursor protein is WT TTR, usually starts to produce clinical cardiac symptoms when patients are more than 80 years old (*10*). ATTR V30M is more prone than WT TTR to undergoing post-translational modification via the Cys residue at position 10. This distinction may contribute to the difference in the time of onset of these two types of systemic amyloidoses.

REFERENCES

1. Pepys, M. B., Hawkins, P. N., Booth, D. R., Vigushin, D. M., Tennent, G. A., Soutar, A. K., Totty, N., Nguyen, O., Blake, C. C., Terry, C. J., Feest, T. G., Zalin, A. M., and Hsuan, J. J. (1993) Human lysozyme gene mutations cause hereditary systemic amyloidosis, *Nature 362*, 553−557.
2. Westermark, P., Bergstrom, J., Solomon, A., Murphy, C., and Sletten, K. (2003) Transthyretin-derived senile systemic amyloidosis: Clinicopathologic and structural considerations, *Amyloid 10*, 48−54.
3. Benson, M. D., and Uemichi, T. (1996) Transthyretin amyloidosis, *Amyloid 3*, 44−56.
4. Ando, Y., Araki, S., and Ando, M. (1993) Transthyretin and familial amyloidotic polyneuropathy, *Intern. Med. (Tokyo, Jpn.) 32*, 920−922.
5. Ando, Y., Nakamura, M., and Araki, S. (2005) Transthyretin related familial amyloidotic polyneuropathy, *Arch. Neurol. 62*, 1−6.
6. Holmgren, G., Steen, L., Suhr, O., Ericzon, B. G., Groth, C. G., Anderson, O., Wallin, B. G., Seymour, A., Richardson, S., Hawkins, P. N., and Pepys, M. B. (1993) Clinical improvement and amyloid regression after liver transplantation in hereditary transthyretin amyloidosis, *Lancet 341*, 1113−1116.
7. Ando, Y., Tanaka, Y., Nakazato, M., Ericzon, B. G., Yamashita, T., Tashima, K., Sakashita, N., Suga, M., Uchino, M., and Ando, M. (1995) Change in variant transthyretin levels in patients with familial amyloidotic polyneuropathy type I following liver transplantation, *Biochem. Biophys. Res. Commun. 211*, 354−358.
8. Ando, Y., Tanaka, Y., Ando, E., Yamashita, T., Nishida, Y., Tashima, Y., Suga, M., Uchino, M., and Ando, M. (1995) Effect of liver transplantation on autonomic dysfunction in familial amyloidotic polyneuropathy type I, *Lancet 345*, 195−196.
9. Skinner, M., Lewis, W. D., Jones, L. A., Kasirsky, J., Kane, K., Ju, S. T., Jenkins, R., Falk, R. H., Simms, R. W., and Cohen, A. S. (1994) Liver transplantation as a treatment for familial amyloidotic polyncuropathy, *Ann. Intern. Med. 120*, 133−134.
10. Cornwell, G. G., III, Sletten, K., Johansson, B., and Westermark, P. (1988) Evidence that the amyloid fibril protein in senile systemic amyloidosis is derived from normal prealbumin, *Biochem. Biophys. Res. Commun. 154*, 648−653.
11. Schoneich, C. (2002) Redox processes of methionine relevant to β-amyloid oxidation and Alzheimer's disease, *Arch. Biochem. Biophys. 397*, 370−376.
12. Rosenblum, W. I. (2002) Structure and location of amyloid β peptide chains and arrays in Alzheimer's disease: New findings require reevaluation of the amyloid hypothesis and of tests of the hypothesis, *Neurobiol. Aging 23*, 225−230.
13. Descamps-Latscha, B., Jungers, P., and Witko-Sarsat, V. (2002) Immune system dysregulation in uremia: Role of oxidative stress, *Blood Purif. 20*, 481−484.
14. Ando, Y., Nyhlin, N., Suhr, O., Holmgren, G., Uchida, K., El-Sahly, M., Yamashita, T., Terasaki, H., Nakamura, M., Uchino, M., and Ando, M. (1997) Oxidative stress is found in amyloid deposits in systemic amyloidosis, *Biochem. Biophys. Res. Commun. 232*, 497−502.
15. Suhr, O., Lang, K., Wikstrom, L., Anan, I., Ando, Y., El-Salhy, M., Holmgren, G., and Tashima, K. (2001) Scavenger treatment of free radical injury in familial amyloidotic polyneuropathy: A study on Swedish transplanted and non-transplanted patients, *Scand. J. Clin. Lab. Invest. 61*, 11−18.
16. Ferdinandy, P. (2004) Nitric oxide and peroxynitrite in cardioprotection: The effect of hyperlipidaemia, *Cardiovasc. J. S. Afr. 15*, S4.
17. Berg, D., Youdim, M. B., and Riederer, P. (2004) Redox imbalance, *Cell Tissue Res. 318*, 201−213.
18. Akaike, T., and Maeda, H. (2000) Nitric oxide and virus infection, *Immunology 101*, 300−308.
19. Kikugawa, K., Hiramoto, K., and Ohkawa, T. (2004) Effects of oxygen on the reactivity of nitrogen oxide species including peroxynitrite, *Biol. Pharm. Bull. 27*, 17−23.
20. McCutchen, S. L., Lai, Z., Miroy, G. J., Kelly, J. W., and Colon, W. (1995) Comparison of lethal and nonlethal transthyretin variants and their relationship to amyloid disease, *Biochemistry 34*, 13527−13536.
21. Kelly, J. W., Colon, W., Lai, Z., Lashuel, H. A., McCulloch, J., McCulloch, S. L., Miroy, G. J., and Peterson, P. A. (1997) Transthyretin quaternary and tertiary structural changes facilitate misassembly into amyloid, *Adv. Protein Chem. 50*, 161−181.
22. Ando, Y., Ohlsson, P. I., Suhr, O., Nyhlin, N., Yamashita, T., Holmgren, G., Danielsson, A., Sansgren, O., Uchino, M., and Ando, M. (1996) A new simple and rapid screening method for variant transthyretin-related amyloidosis, *Biochem. Biophys. Res. Commun. 228*, 480−483.
23. Kishikawa, M., Nakanishi, T., Miyazaki, A., Shimizu, A., Kusaka, H., Fukui, M., and Nishiue, T. (1999) A new amyloidogenic transthyretin variant, [D38A], detected by electrospray ionization/mass spectrometry, *Amyloid 6*, 183−186.
24. Takaoka, Y., Ohta, M., Miyakawa, K., Nakamura, O., Suzuki, M., Takahashi, K., Yamamura, K., and Sakaki, Y. (2004) Cysteine 10 is a key residue in amyloidogenesis of human transthyretin Val30Met, *Am. J. Pathol. 164*, 337−345.
25. Zhang, Q., and Kelly, J. W. (2003) Cys10 mixed disulfides make transthyretin more amyloidogenic under mildly acidic conditions, *Biochemistry 42*, 8756−8761.
26. Sousa, M. M., Fernandes, R., Palha, J. A., Taboada, A., Vieira, P., and Saraiva, M. J. (2002) Evidence for early cytotoxic aggregates in transgenic mice for human transthyretin Leu55Pro, *Am. J. Pathol. 161*, 1935−1948.
27. Ando, Y., Yamashita, T., Nakamura, M., Tanaka, Y., Hashimoto, M., Tashima, K., Suhr, O., Uemura, Y., Obayashi, K., Terazaki, H., Suga, M., Uchino, M., and Ando, M. (1997) Down regulation of a harmful variant protein by replacement of its normal protein, *Biochim. Biophys. Acta 1362*, 39−46.
28. Hermansen, L. F., Bergman, T., Jornvall, H., Husby, G., Ranlov, I., and Sletten, K. (1995) Purification and characterization of amyloid-related transthyretin associated with familial amyloidotic cardiomyopathy, *Eur. J. Biochem. 227*, 772−779.
29. Quintas, A., Saraiva, M. J., and Brito, R. M. (1997) The amyloidogenic potential of transthyretin variants correlates with their tendency to aggregate in solution, *FEBS Lett. 418*, 297−300.
30. Miyamoto, Y., Akaike, T., and Maeda, H. (2000) S-Nitrosylated human α_1-protease inhibitor, *Biochim. Biophys. Acta 1477*, 90−97.
31. Akaike, T. (2000) Mechanisms of biological S-nitrosation and its measurement, *Free Radical Res. 33*, 461−469.
32. Inoue, K., Akaike, T., Miyamoto, Y., Okamoto, T., Sawa, T., Otagiri, M., Suzuki, S., Yoshimura, T., and Maeda, H. (1999) Nitrosothiol formation catalyzed by ceruloplasmin. Implication for cytoprotective mechanism in vivo, *J. Biol. Chem. 274*, 27069−27075.
33. Takabayashi, K., Imada, T., Saito, Y., and Inada, Y. (1983) Coupling between fatty acid binding and sulfhydryl oxidation in bovine serum albumin, *Eur. J. Biochem. 136*, 291−295.
34. Akaike, T., Inoue, K., Okamoto, T., Nishino, H., Otagiri, M., Fujii, S., and Maeda, H. (1997) Nanomolar quantification and identification of various nitrosothiols by high performance liquid chromatography coupled with flow reactors of metals and Griess reagent, *J. Biochem. 122*, 459−466.
35. Saville, B. (1958) A scheme for the colorimetric determination of microgram amounts of thiols, *Analyst 83*, 670−672.

36. Goldberg, M. E., Rudolph, R., and Jaenicke, R. (1991) A kinetic study of the competition between renaturation and aggregation during the refolding of denatured-reduced egg white lysozyme, *Biochemistry 30*, 2790−2797.
37. Bonifacio, M. J., Sasaki, Y., and Saraiva, M. J. (1996) 'In vitro' amyloid fibril formation from transthyretin: The influence of ions and the amyloidogenicity of TTR variants, *Biochim. Biophys. Acta 1316*, 35−42.
38. Naiki, H., Higuchi, K., Hosokawa, M., and Takeda, T. (1989) Fluorometric determination of amyloid fibrils in vitro using the fluorescent dye, thioflavin T1, *Anal. Biochem. 177*, 244−249.
39. del Rio, L. A., Corpas, F. J., Sandalio, L. M., Palma, J. M., Gomez, M., and Barroso, J. B. (2002) Reactive oxygen species, antioxidant systems and nitric oxide in peroxisomes, *J. Exp. Bot. 53*, 1255−1272.
40. Mirza, U. A., Chait, B. T., and Lander, H. M. (1995) Monitoring reactions of nitric oxide with peptides and proteins by electrospray ionization-mass spectrometry, *J. Biol. Chem. 270*, 17185−17188.
41. Skinner, M., Stone, P., Shirahama, T., Connors, L. H., Calore, J., and Cohen, A. S. (1986) The association of an elastase with amyloid fibrils, *Proc. Soc. Exp. Biol. Med. 181*, 211−214.
42. Jiang, X., Buxbaum, J. N., and Kelly, J. W. (2001) The V122I cardiomyopathy variant of transthyretin increases the velocity of rate-limiting tetramer dissociation, resulting in accelerated amyloidosis, *Proc. Natl. Acad. Sci. U.S.A. 98*, 14943−14948.
43. Jaffrey, S. R., Erdjument-Bromage, H., Ferris, C. D., Tempst, P., and Snyder, S. H. (2001) Protein S-nitrosylation: A physiological signal for neuronal nitric oxide, *Nat. Cell Biol. 3*, 193−197.
44. Foster, M. W., McMahon, T. J., and Stamler, J. S. (2003) S-nitrosylation in health and disease, *Trends Mol. Med. 9*, 160−168.
45. Jia, L., Bonaventura, C., Bonaventura, J., and Stanler, J. S. (1996) S-nitrosohaemoglobin: A dynamic activity of blood involved in vascular control, *Nature 380*, 221−226.

BI050327I

Available online at www.sciencedirect.com
SCIENCE DIRECT®
Biochemical and Biophysical Research Communications 334 (2005) 1322–1328
BBRC
www.elsevier.com/locate/ybbrc

The structure and function of oxidized albumin in hemodialysis patients: Its role in elevated oxidative stress via neutrophil burst

Katsumi Mera [a,1], Makoto Anraku [a,1], Kenichiro Kitamura [b], Keisuke Nakajou [a], Toru Maruyama [a], Masaki Otagiri [a,*]

[a] *Department of Biopharmaceutics, Graduate School of Pharmaceutical Sciences, Kumamoto University, Kumamoto 862-0973, Japan*
[b] *Department of Nephrology, Graduate School of Medical Sciences, Kumamoto University, Kumamoto 860-8655, Japan*

Received 3 July 2005
Available online 18 July 2005

Abstract

Oxidized albumin is a reliable marker of oxidative stress in hemodialysis (HD) patients. However, oxidized albumin in vivo and its possible clinical significance has been rarely investigated. In the present study, the qualitative modification of albumin in HD patients ($n = 20$) was examined and their results were compared with healthy age-matched controls ($n = 10$). The increase in plasma protein carbonyl levels in HD patients was largely due to an increase in oxidized albumin. Human serum albumin (HSA) of HD patients, HSA of HD patients (HD-HSA) and normal subjects (Normal-HSA) were purified on a blue Sepharose CL-6B column. Spectroscopic analysis confirmed that the HD-HSA samples contained higher levels of carbonyls than Normal-HSA. An HPLC analysis also suggested that the state of the purified HSA used throughout the experiments accurately reflects the redox state of albumin in blood. HD-HSA was found to have a decreased the antioxidant activity, and was able to trigger the oxidative burst of human neutrophils, compared to Normal-HSA. HD-HSA was conformationally altered, with its hydrophobic regions more exposed and to have a negative charge. In binding experiments, HD-HSA showed impaired Site II-ligand binding capabilities. Collectively, the oxidation of plasma proteins, especially HSA, might enhance oxidative stress in HD patients.

Keywords: Human serum albumin; Oxidation; Neutrophil burst; Hemodialysis patients; Carbonyl groups; Conformational changes; Hydrophobicity; Net charge; Ligand binding; HPLC analysis

The oxidative modification of proteins and lipids has been implicated in the etiology of numerous disorders and diseases [1,2]. Oxidatively modified plasma proteins can serve as important in vivo biomarkers of oxidative stress. Proteins are better candidates than plasma lipids for use in detecting specific pathways of oxidative stress, due to the accessibility of plasma protein for sampling, their relatively long half-lives, and their well-defined biochemical pathways.

Since extracellular fluids contain only small amounts of antioxidant enzymes, it has been proposed that the major extracellular antioxidants are proteins and circulating albumin is a major antioxidant in plasma [3]. The in vitro oxidation of amino acid residues leads to protein degradation, aggregation, and cross-linking. In contrast, significant evidence for the presence of ROS-mediated protein damage in vivo and its possible clinical significance is not currently available. Witko-Sarsat et al. [4] reported the presence of elevated levels of oxidized protein products, termed advanced oxidation protein products (AOPP) such as oxidized albumin, in the plasma of dialysis patients. It has been well documented that human serum albumin (HSA) is quite vulnerable to reactive oxygen species (ROS) [5]. Therefore, HSA is continuously exposed to oxidative stress, so that alterations of the conformation and function of HSA could

* Corresponding author. Fax: +81 96 362 7690.
E-mail address: otagirim@gpo.kumamoto-u.ac.jp (M. Otagiri).
[1] These two authors contributed equally to this work.

0006-291X/$ - see front matter © 2005 Elsevier Inc. All rights reserved.
doi:10.1016/j.bbrc.2005.07.035

occur, resulting in modification of its biological properties.

In recent years, activated phagocytes have been reported to be a major source of reactive oxidants and to play a fundamental role in host defense [6,7]. They contain the heme enzyme myeloperoxidase (MPO) which catalyzes the reaction of chloride ion with hydrogen peroxide (H_2O_2) to generate large amounts of hypochlorous acid (HOCl), a powerful oxidizing and chlorinating agent produced by neutrophils [8–10]. Treatment of HSA with HOCl in vitro and in vivo-generated AOPP have been reported to trigger oxidative bursts in neutrophils as well as in monocytes, thereby appearing to act as true inflammatory mediators [11,12]. The possibility that excessively oxidized albumin in plasma increases the production of ROS by stimulating neutrophils, cannot be excluded. Therefore, very excessively oxidized HSA, could also play an important role as a pro-oxidant in dialysis patients.

We previously demonstrated that oxidative stress in HD patients is manifested by an increase in plasma protein oxidation that is characterized by thiol group oxidation and the formation of carbonyl groups on proteins. We also showed that HSA is the major plasma protein target of oxidative stress in uremia, and that increased levels of carbonyl compounds are correlated with the oxidation of albumin in uremic patients [13]. Therefore, serum albumin is an important protein that has direct protective effects. These effects may be also based on a variety of biological mechanisms. In the present study, we further investigated the role of albumin oxidation and neutrophil oxidative burst in HD patients and compared the results with age- and gender-matched control subjects. An evaluation of the effects of oxidative stress on the structural and functional properties of HSA was also attempted.

Materials and methods

Patients

The protocol used in this study was approved by the institutional review board and informed consent was obtained from all subjects. A total of 30 subjects were enrolled: 20 stable HD patients (10 men, 10 women) aged 36–87 years, with a duration of dialysis ranging from 1 to 9 years, and 10 age- and gender-matched healthy control subjects. End-stage renal failure in HD patients was caused by glomerulonephritis ($n = 5$), nephrosclerosis ($n = 2$) or diabetic nephropathy ($n = 13$). At the time of enrollment, all HD patients had been receiving regular bicarbonate hemodialysis therapy (4–5 h/session, three times per week) using high-flux polysulfone hollow-fiber dialyzers. The profiles of healthy controls and HD patients with or without diabetes are summarized in Table 1.

Table 1
Characteristics of the normal and patient groups

	Normal subjects ($N = 10$)	HD patients ($N = 20$)
Age (years)	67.8 ± 1.8	62.8 ± 12.7
Gender (M/F)	6/4	10/10
Diabetes/nondiabetes	—	13/7
Creatinine (mg/dL)	0.85 ± 0.2	10.6 ± 2.6*

Values are expressed means ± SD.
* $P < 0.01$.

Purified albumin from healthy control and HD patients

HSA samples were isolated by polyethylene glycol fractionation of blood plasma followed by chromatography on a blue Sepharose CL-6B column (Amersham-Pharmacia, Uppsala, Sweden) [14]. The samples were then dialyzed against deionized water for 48 h at 4 °C, followed by lyophilization. The purity of the HSA samples was at least 95%, and the percentage of dimers did not exceed 7%, as evidenced by SDS–PAGE and native-PAGE, respectively. The long-chain fatty acid contents of isolated HSA samples were determined using the copper triethanolamine method [15]. There was no significant change of the long-chain fatty acid contents in purified albumin from healthy controls and HD patients.

Determination of serum protein and purified albumin oxidation

Chromatographic analysis of albumin in normal subjects and HD patients. HSA is a mixture of mercaptalbumin (HMA; reduced form) and nonmercaptalbumin (HNA; oxidized form). HMA contains one highly reactive sulfhydryl group at position 34 (Cys-34), while other serum proteins contain little or none. HNA is comprised of at least three types of molecules. The major HNA component is a mixed disulfide with cysteine or glutathione (HNA-1). The other is a more highly oxidized product than the mixed disulfide, in which the thiol group has been oxidized to the sulfenic (SOH), sulfinic (SO_2H), and sulfonic (SO_3H) states (HNA-2), the proportions of which are extremely small in extracellular fluids [16,17]. The high-performance liquid chromatography (HPLC) analysis of albumin developed by Sogami et al. permits the clean separation of HSA into HMA and HNA, and is used for the determination of the redox state for various pathophysiologic conditions. An HPLC analysis of serum albumin was performed as described in a previous report [13]. Serum samples were immediately frozen immediately after they were drawn, and were stored at −80 °C until used for HPLC. HPLC was performed using 5 μL aliquots of each serum sample and a Shodex Asahipak ES-502N column (Showa Denko, Tokyo, Japan; column temperature; 35 ± 0.5 °C). The HPLC system consisted of an L-6200 intelligent pump equipped with a gradient programmer and an F-1050 fluorescence detector (Jasco, Tokyo, Japan). Elution was performed using a linear gradient with ethanol concentrations increasing from 0% to 5% with the serum dissolved in a mixture of 0.05 mol/L sodium acetate and 0.40 mol/L sodium sulfate (pH 4.85) at a flow rate of 1.0 mL/min. From the HPLC profiles of HSA, the value of each albumin fraction [f(HMA), f(HNA-1), and f(HNA-2)] was estimated by dividing the area of each fraction by the total area corresponding to HSA.

Total plasma protein and individual plasma carbonyl contents measurement. Plasma protein carbonyl content was determined using the method of Climent et al. [18].

Biological properties of Normal- and HD-HSA

Radical scavenging ability of Normal- and HD-HSA. The radical scavenging activity of Normal- and HD-HSA (10 μM) was determined from the decrease in the absorbance of 1,1′-diphenyl-2-picrylhydrazyl (DPPH) radicals at 517 nm due to their scavenging of an unpaired electron of the stable DPPH radical in a mixture of 10 mL ethanol, 10 mL of 50 mM 2-(*N*-morpholino)ethanesulfonic acid (Mes) buffer (pH 5.5), and 5 mL of 0.5 mM DPPH in ethanol [19–21].

Measurement of neutrophil respiratory burst. Neutrophils were isolated from heparinized peripheral blood of healthy donors using Lymphoprep (Nycomed, Oslo, Norway) density gradient centrifugation. The purity of the PMN preparations routinely exceeded 95%, and cell viability, as determined by propidium iodide staining, was at least 98%. Accumulation of dihydrorhodamine 123 (DRD) in a suspension of neutrophils was measured using a flow cytometer, monitoring the fluorescence at 526 nm [22]. Suspensions of neutrophils (1×10^6 cells) were incubated with 5 μM DRD for 15 min at 37 °C in serum-free medium. After DRD incubation, the neutrophil suspension was centrifuged and washed to remove unincorporated probe. The cells were then treated with various concentrations of albumin medium for 1 h at 37 °C, and were then placed on ice. The mean fluorescence intensity of rhodamine (RD) in the cells was determined using a flow cytometer (FACS Calibur; Becton–Dickinson Biosciences, Franklin Lakes, NJ).

Structural and functional properties of Normal- and HD-HSA

CD measurements. These measurements were performed using a Jasco J-720 type spectropolarimeter (Jasco, Tokyo, Japan) at 25 °C. Far-UV spectra were recorded at a protein concentration of 20 μM in 67 mM sodium phosphate buffer (pH 7.4) using 1 mm quartz cells.

Effective protein hydrophobicity. The effective hydrophobicity of all the albumins (1 μM), dissolved in a 67 mM sodium phosphate buffer (pH 7.4), was probed with 4,4′-dianilino-1,1′-binaphthyl-5,5′-disulfonic acid (bis-ANS) (10 μM) at 25 °C. The compound was excited at 394 nm and fluorescence spectra were recorded on a Jasco FP-770 fluorescence spectrometer (Tokyo, Japan) using 1 cm quartz cells.

Changes in protein net charge. Changes in the net charge of albumin were evaluated by a modification of the capillary electrophoresis method described by Pande et al. [23]. One milliliter of an HSA sample (2 μM) was run in 100 mM borate buffer (pH 8.5 and 20 °C), and the migration time was determined by capillary electrophoresis, model CE990/990-10 from Jasco (Tokyo, Japan).

Binding properties. The binding of warfarin (5 μM) and ketoprofen (5 μM) to purified HSA (10 μM) in 67 mM sodium phosphate buffer (pH 7.4 and 25 °C) was examined by ultrafiltration. The unbound ligand fractions were separated using an Amicon MPS-1 micropartition system with YMT ultrafiltration membranes by centrifugation (2000*g*, 40 min). The concentration of unbound ligand was determined by HPLC [14]. The unbound fraction (%) was calculated as follows:

$$\text{Unbound fraction}(\%) = [\text{ligand concentration in filtered fraction}/\text{total ligand concentration(before ultrafiltration)}] \times 100.$$

Statistics

The statistical significance of collected data was evaluated using the ANOVA analysis followed by Newman–Keuls method for more than 2 means. A value of $P < 0.05$ was considered to indicate statistical significance. The results are reported as the mean ± SD.

Results

Determination of serum protein and purified albumin oxidation

The oxidation of a protein typically results in an increase in carbonyl content. This increase is due to the oxidation of Lys, Arg, or Pro residues. Plasma protein carbonyl contents were significantly increased in HD patients, compared with normal subjects. Data for the carbonyl content were as follows: HD patients groups, 3.12 ± 1.11 nmol/mg protein, $n = 20$; controls groups, 2.1 ± 0.34 nmol/mg protein, $n = 10$ ($P < 0.01$) (Table 2). In a previous study, we determined the redox states of HD patients during oxidative stress, with emphasis on the oxidation of serum albumin [13]. In the present study, using HPLC, we determined the oxidation status of the Cys-34 residues in albumin. Table 2 shows typical HPLC profiles for serum albumin from healthy subjects and HD patients. f(HMA) was substantially decreased and both f(HNA-1) and f(HNA-2) were significantly increased in HD patients compared with healthy subjects ($P < 0.01$, Table 2). These results suggest that uremia results in an increase in the oxidized serum albumin levels, via oxidative stress.

Further, to investigate the extent of alterations in the biological properties of HSA in HD patients, HSA of HD patients (HD-HSA), and normal subjects (Normal-HSA) were purified on a blue Sepharose CL-6B column. The albumin carbonyl contents of the purified fraction were significantly increased in HD patients. Data for the carbonyl content of purified HSA were as follows: HD-HSA, 2.86 ± 0.45 nmol/mg protein, $n = 20$; Normal-HSA, 2.13 ± 0.14 nmol/mg protein, $n = 10$, $P < 0.01$ (Table 2). HD-HSA samples also showed a markedly increased HNA ratio, compared with Normal-HSA ($P < 0.01$, Table 2). In addition, the HNA/HMA ratio of purified HSA was closely correlated with the HNA/HMA of plasma ($R = 0.952$, $P < 0.01$;

Table 2
Determination of serum protein and purified albumin oxidation

	Serum protein		Purified HSA	
	Normal subjects	HD patients	Normal-HSA	HD-HSA
Carbonyl contents (nmol/mg protein)	2.10 ± 0.34	3.12 ± 1.11*	2.13 ± 0.14	2.86 ± 0.45**
f(HMA) (%)	53.6 ± 6.4	40.4 ± 8.7*	46.6 ± 4.9	32.7 ± 6.8**
f(HNA-1) (%)	38.7 ± 6.3	49.7 ± 8.0*	42.0 ± 4.4	54.4 ± 7.1**
f(HNA-2) (%)	7.7 ± 0.9	9.9 ± 1.4*	11.4 ± 0.3	12.9 ± 0.7**

Values are expressed means ± SD.
* $P < 0.01$ as compared with Normal subjects.
** $P < 0.01$ as compared with Normal-HSA.

data not shown). These results suggest that the state of purified HSA accurately reflects the redox state of albumin in the blood.

Physiological properties of Normal- and HD-HSA

Radical scavenging ability of Normal- and HD-HSA

The effects of Normal- and HD-HSA were examined by monitoring the time-dependent change in the absorbance of DPPH radicals. As shown in Fig. 1, Normal-HSA scavenged DPPH radicals, and its ability to scavenge proceeded more fastly than HD-HSA. HD-HSA scavenged about 15% of DPPH radicals even after 20 min. In contrast, the effect of Normal-HSA proceeded more rapidly, about 20% of the DPPH radicals were scavenged within 20 min. This result shows that the radical scavenging activity of Normal-HSA was significantly greater than that of HD-HSA.

Neutrophil respiratory burst

It was recently reported that in vitro-oxidized albumin up-regulates ROS generation in neutrophil suspensions [4]. In order to directly assess whether purified HSA had the ability to induce oxidative stress in a neutrophil suspension, we used the DRD method and a FACS analysis. The levels of ROS were higher for HD-HSA than for Normal-HSA (Fig. 2) ($P < 0.05$). These results show that HD-HSA was not able to decrease the antioxidant activity, but also to trigger the oxidative burst of human neutrophils.

Structural and functional properties of Normal- and HD-HSA

Structural properties of Normal- and HD-HSA

The structural properties of Normal- and HD-HSA were examined by a variety of methods. Thus, Fig. 3A shows Far-UV CD spectra. As can be seen in Fig. 3A, the characteristics of the CD spectrum of HD-HSA were slightly different from that obtained for Normal-HSA. The effect of oxidation on the exposure of hydrophobic areas was also examined by using the fluorescence probe bis-ANS. The results obtained (Fig. 3B) indicate that the conformation of HD-HSA in particular, involves an increase in accessible hydrophobic regions, compared with Normal-HSA. The net charges of HD- and Normal-HSA were investigated by determining their migration times in capillary electrophoresis. The migration time for HD-HSA (25.65 ± 0.52 min) was increased slightly compared with that of Normal-HSA (24.84 ± 0.46 min) ($P < 0.01$). These results suggest that HD-HSA also underwent conformational changes, hydrophobic regions were more exposed and negative charge on the molecule was increased.

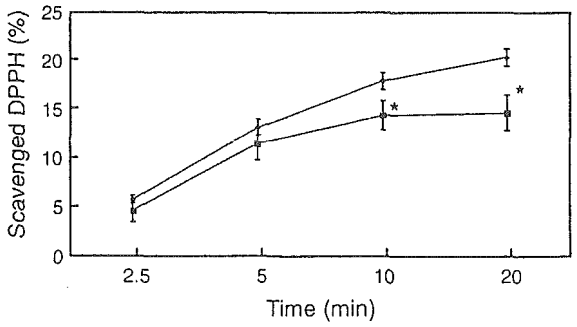

Fig. 1. Radical scavenging ability of Normal- and HD-HSA. Normal- and HD-HSA at a final concentration of 20 μM were added to a suspension of ethanol, in which DPPH radicals were incorporated (final concentration of 20 μM), in 175 mM KCl and 10 mM Mes buffer (pH 7.4) at 25 °C. Changes in the amount of DPPH radicals in the suspension were monitored as a decrease in absorbance at 517 nm. Changes in DPPH radicals scavenged relative to total DPPH radicals with time are shown. *$P < 0.05$, compared with Normal-HSA.

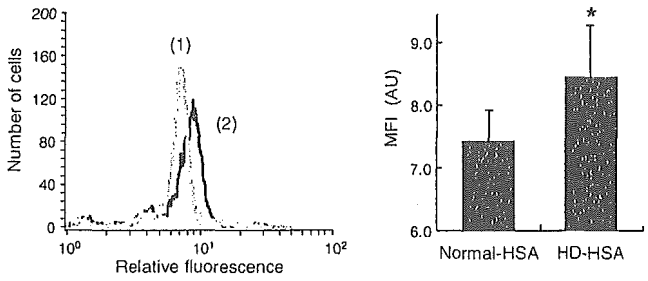

Fig. 2. ROS production by neutrophils incubated with purified HSA. (1) Normal-HSA, (2) HD-HSA. *$P < 0.05$, compared with Normal-HSA.

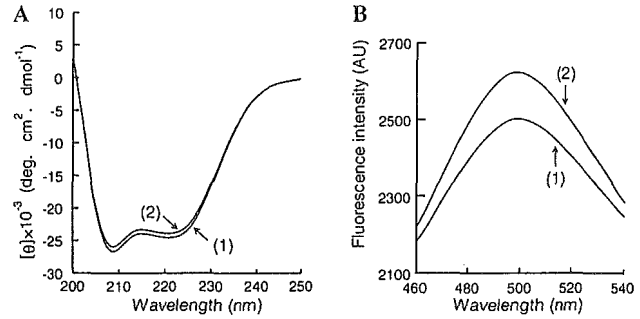

Fig. 3. (A) Purified HSA far-UV CD spectra of normal subjects and HD patients. (1) Normal-HSA, (2) HD-HSA. The spectra are the average of three determinations. (B) Effect of uremia on the fluorescence of purified HSA-bound bis-ANS. (1) Normal-HSA, (2) HD-HSA. The spectra are the average of three determinations.

Binding property of Normal- and HD-HSA

The unique ligand binding properties of HSA can, to a great extent, be explained by the presence of two major binding sites, Site I and Site II [24], which are located within specialized cavities in subdomains IIA and IIIA, respectively [25]. The potential effect of oxidation on these sites was examined by using warfarin and ketopro-

fen as representative ligands. As seen from Table 3, the high-affinity binding of warfarin, which takes place at Site I [26] was little changed, but the high affinity binding of the Site II-ligand ketoprofen [27] was significantly reduced in HD-HSA, compared with Normal-HSA.

Discussion

Apart from the low-molecular weight antioxidants, the antioxidant activity in human blood plasma relies mainly on proteins such as albumin [28]. In plasma, the free thiol group is quantitatively the most important scavenger of oxidants. Furthermore, the formation of carbonyl groups in plasma albumin, as previously demonstrated by Himmelfarb and Mcmonagle [28], involves in basic amino acid residues as well as Cys-34 with free thiol group, which is also oxidized. In the previous study, using a Western blot immunoassay, we demonstrated that the carbonylation of albumin accounts for nearly all of the excess plasma protein oxidation in HD patients [13]. We also found that the f(HMA) value in albumin from HD patients was less than 80% of the f(HMA) value in albumin from healthy controls, as indicated by HPLC analysis (Table 2). Since albumin is the most abundant plasma protein, it could play a major role as an antioxidant in plasma at least by thiol oxidation and carbonyl formation. In this context, we expected that the characterization of oxidation status of serum albumin would provide, not only useful information regarding the redox state of the human body, but also alterations in the conformation and function of HSA which may result in modifications of its biological properties.

In HD patients with increased oxidative stress, the oxidative modification of plasma proteins especially albumin appear to be more extensive and may be one of the pathological conditions associated with the widespread vascular complications that are frequently observed in HD patients. To investigate the extent of the alterations in the biological properties of HSA in HD patients, HSA from HD patients (HD-HSA) and normal subjects (Normal-HSA) were purified with blue Sepharose CL-6B column chromatography. The retention time and chromatogram of the purified albumin and plasma albumin were found to be highly correlated (Table 2). Thus, the HNA/HMA ratio of purified HSA can be used as an index for the HNA/HMA ratio of plasma ($R = 0.952$, $P < 0.01$). The high correlation between the HNA/HMA value of plasma and purified HSA suggest that the state of purified HSA used throughout the experiments accurately reflects the redox state of albumin in the blood.

We first focused on the antioxidant activity of albumin because oxidative stress is thought to play a significant role in the pathogenesis of many diseases, including atherosclerosis [29,30]. There is now ample evidence to suggest that albumin, as the main circulating protein, is a quantitatively important antioxidant in the blood and extracellular fluids [31,32]. Our present studies are in full agreement with this view, Normal-HSA offered significant protection against free radicals, compared to HD-HSA (Fig. 1). These antioxidant effects were found to be concentration-dependent (data not shown), consistent with a beneficial effect of high albumin levels in humans. This in turn suggests that excessively oxidized albumin, which acts as a pro-oxidant, may increase cardiovascular complications in HD patients. In these patients recurrent blood interactions with bioincompatible dialysis membranes trigger neutrophil activation and the subsequent generation of highly reactive oxygen species (ROS) including O_2^- and its derivatives (H_2O_2, $OH^{\cdot}$, and $^1O_2$) via the nicotinamide adenine dinucleotide phosphate (NADPH) oxidase complex and OCl via a MPO-dependent reaction between chloride and H_2O_2 [4]. To test the hypothesis that the increased oxidative stress in blood of HD patients is caused by oxidized albumin, we examined the effects of incubating neutrophils with purified albumin from Normal- or HD-HSA. Purified albumin from HD patients (HD-HSA) induced oxidative stress via a neutrophil respiratory burst (Fig. 2). In previous studies, excess AOPP-modified albumin, was found to be associated with a high level of respiratory burst [12], but the samples used in those studies were produced by chemical modification in vitro. In the present studies, HD-HSA, isolated from uremia patients was found to have been modified in vivo. Treatment of neutrophils with purified albumin from HD patients induced oxidative stress. Therefore, HD-HSA was, found not only to have a decreased antioxidant activity, but also able to trigger the oxidative burst of human neutrophils, compared with Normal-HSA.

These results suggest that HSA is continuously exposed to oxidative stress, so much so that alterations in its biological properties that could result in the conformational, functional changes of HSA occur. Therefore, the significance of conformational changes of purified HSA on its functional properties were examined. Slight decreases in α-helical content accompanied by tertiary conformational changes were observed for HD-HSA (data not shown). These changes, which could

Table 3
Binding of warfarin and ketoprofen to Normal-HSA and HD-HSA

	Free fraction (%)	
	Warfarin	Ketoprofen
Normal-HSA	19.6 ± 1.9	5.97 ± 0.75
HD-HSA	23.3 ± 2.0	9.37 ± 1.36*

Values are expressed means ± SD.
* $P < 0.05$.

be observed by near-UV CD resulted in an increased exposure of hydrophobic regions of the protein (Fig. 3). Changes in net charge on the HSA surface were also observed. These results suggest that the increase of negative charge reflects oxidation of basic amino acid residues in albumin. In plasma, all amino acids in the protein are susceptible to oxidative modification by oxidants such as hydroxyl radicals and hypochlorous acid. Among them, amino acids such as cysteine, histidine, lysine, and arginine are more vulnerable to oxidation [33]. Modification of these residues results in conformational changes in cases of uremia.

The high-affinity binding of warfarin and ketoprofen was studied in order to determine whether the drug binding properties of HSA had been affected by uremia. In this experiment, the drug binding properties of HD-HSA were found to be reduced. The decreased ketoprofen binding to HD-HSA is most probably caused by conformational changes involving Site II in subdomain IIIA [24]. The decreased binding to HD-HSA might be also caused by the oxidation of ^{410}Arg. Ahmed et al. [34] recently suggested that ^{410}Arg is a target site for oxidative stress. Using an anti-carboxyl methyl-Lysine and an anti-hydro-imidazolone antibody to identify advanced glycation endproducts, we also found that HD-HSA could be recognized by this antibody. This indicates that Lys and Arg residues in HD-HSA were modified (data not shown), causing structural changes due to oxidative stress in HD patients. In addition, this alteration may further aggravate the pre-existing elevated concentration of unbound free drugs in HD patients. Therefore, the structural alteration of HSA in uremia results in the loss of some important properties of HSA.

In conclusion, the present study has shown that the oxidative modification of HSA in HD patients may lead to alterations in the conformation as well as the biological properties of HSA. The present study further propose that, in addition to its serum concentration, the quality of HSA molecules may be not only a crucial factor affecting its protective effects but also a risk factor as a pro-oxidant in HD patients. The present study provides evidence to suggest that isolated HSA in hemodialyzed patients has, not only reduced structural and functional properties, but also acts as a mediator of the neutrophil activation state associated with chronic uremia.

Acknowledgments

Authors thank Dr. Shunichi Sakaguchi (Midorigaoka Clinic, Kumamoto, Japan) for blood sample collection from HD patients.This work was supported by the Grants-in-Aid for Scientific Research from the Ministry of Education, Culture, Sports, Science and Technology in Japan (15790432 to K.K., 14370759 and 14657618 to M.O.), the Salt Science Research Foundation (0330 to K.K.), and Japan Heart Foundation Research Grant (to K.K.)

References

[1] F.G. Njoroge, L.M. Sayre, V.M. Monnier, Detection of glucose-derived pyrrole compounds during Maillard reaction under physiological conditions, Carbohydr. Res. 167 (1987) 211–220.
[2] J.W. Baynes, V.M. Monnier, The Maillard reaction in aging, diabetes and nutrition, Prog. Clin. Biol. Res. 304 (1989) 1–410.
[3] J.P. Domeiko, D.J. Nompleggi, Role of albumin in human physiology and pathophysiology, J. Parenter. Enteral Nutr. 15 (1991) 207–211.
[4] V. Witko-Sarsat, M. Friedlander, T. Nguyen Khoa, C. Capeillere-Blandin, A.T. Nguyen, S. Canteloup, J.M. Dayer, P. Jungers, T. Drueke, B. Descamps-Latscha, Advanced oxidation protein products as novel mediators of inflammation and monocyte activation in chronic renal failure, J. Immunol. 161 (1998) 2524–2532.
[5] K.J.A. Davies, Protein damage and degradation by oxygen radicals, J. Biol. Chem. 262 (1987) 9895–9901.
[6] S.J. Klebanoff, Oxygen metabolites from phagocytes, in: J.L. Gallin, R. Snyderman (Eds.), Inflammation: Basic Principles and Clinical Correlates, Lippincott Williams & Wilkins, Philadelphia, 1999, pp. 721–768.
[7] J. Odajima, M. Onishi, Biological significance and mechanisms of reactions and events mediated by myeloperoxidase in the xenobiotic metabolism and disposition pathways of leucocytes, Med. Sci. Res. 26 (1998) 291–298.
[8] H.B. Dunford, Myeloperoxidase and eosinophil peroxidase: phagocytosis and microbial killing, in: Heme Peroxidases, Wiley, New York, 1999, pp. 349–385.
[9] A.J. Kettle, C.C. Winterbourn, Myeloperoxidase: a key regulator of neutrophil oxidant production, Redox Rep. 3 (1997) 3–15.
[10] J.P. Eiserich, M. Hristova, C.E. Cross, A.D. Jones, B.A. Freeman, B. Halliwell, A. van der Vliet, Formation of nitric oxide-derived inflammatory oxidants by myeloperoxidase in neutrophils, Nature 391 (1998) 393–397.
[11] B. Descamps-Latscha, V. Witko-Sarsat, Importance of oxidatively modified proteins in chronic renal failure, Kidney Int. 59 (2001) S108–S113.
[12] V. Witko-Sarsat, V. Gausson, A.T. Nguyen, M. Touam, F. Santangelo, B. Descamps-Latscha, AOPP-induced activation of human neutrophil and monocyte oxidative metabolism: a potential target for *N*-acetyl-cysteine treatment in dialysis patients, Kidney Int. 64 (2003) 82–91.
[13] M. Anraku, K. Kitamura, A. Shinohara, M. Adachi, A. Suenaga, T. Maruyama, K. Miyanaka, T. Miyoshi, N. Shiraishi, H. Nonoguchi, M. Otagiri, K. Tomita, Intravenous iron administration induces oxidation of serum albumin in hemodialysis patients, Kidney Int. 66 (2004) 841–848.
[14] H. Watanabe, K. Yamasaki, U. Kragh-Hansen, S. Tanase, K. Harada, A. Suenaga, M. Otagiri, In vitro and in vivo properties of recombinant human serum albumin from *Pichia pastoris* purified by a method of short processing time, Pharm. Res. 18 (2001) 1775–1781.
[15] W.G. Duncombe, The colorimetric micro-determination of non-esterified fatty acid in plasma, Clin. Chim. Acta 10 (1964) 122–125.
[16] M. Sogami, S. Nagoka, S. Era, M. Honda, K. Noguchi, Resolution of human mercapt- and nonmercaptalbumin by high-performance liquid chromatography, Int. J. Pept. Protein Res. 24 (1984) 96–103.
[17] S. Era, T. Hamaguchi, M. Sogami, K. Kuwata, E. Suzuki, K. Miura, K. Kawai, Y. Kitazawa, H. Okabe, A. Noma, Further

studies on the resolution of human mercapt- and nonmercaptalbumin and on human serum albumin in the elderly by high-performance liquid chromatography, Int. J. Pept. Protein Res. 3 (1985) 435–442.
[18] I. Climent, L. Tsai, R.L. Levine, Derivatization of gamma-glutamyl semialdehyde residues in oxidized proteins by fluoresceinamine, Anal. Biochem. 182 (1989) 226–232.
[19] H. Sassa, Y. Takaishi, H. Terada, The triterpene celastrol as a very potent inhibitor of lipid peroxidation in mitochondria, Biochem. Biophys. Res. Commun. 172 (1990) 890–897.
[20] H. Sassa, K. Kogure, Y. Takaishi, H. Terada, Structural basis of potent antiperoxidation activity of the triterpene celastrol in mitochondria: effect of negative membrane surface charge on lipid peroxidation, Free Radic. Biol. Med. 17 (1994) 201–207.
[21] K. Kogure, S. Goto, K. Abe, C. Ohiwa, M. Akasu, H. Terada, Potent antiperoxidation activity of the bisbenzylisoquinoline alkaloid cepharanthine: the amine moiety is responsible for its pH-dependent radical scavenge activity, Biochim. Biophys. Acta 1426 (1999) 133–142.
[22] H. Nakajima, M. Takenaka, J.Y. Kaimori, T. Hamano, H. Iwatani, T. Sugaya, T. Ito, M. Hori, E. Imai, Activation of the signal transducer and activator of transcription signaling pathway in renal proximal tubular cells by albumin, J. Am. Soc. Nephrol. 15 (2004) 276–285.
[23] P.G. Pande, R.V. Nellore, H.R. Bhagat, Optimization and validation of analytical conditions for bovine serum albumin using capillary electrophoresis, Anal. Biochem. 204 (1992) 103–106.
[24] G. Sudlow, D.J. Birkett, D.N. Wade, The characterization of two specific drug binding sites on human serum albumin, Mol. Pharmacol. 11 (1975) 824–832.
[25] D.C. Carter, J.X. Ho, Structure of serum albumin, Adv. Protein Chem. 45 (1994) 153–203.
[26] T. Peters Jr, All about Albumin, Biochemistry, Genetics, and Medical Applications, Academic Press, San Diego, 1996.
[27] V.T.G. Chuang, A. Kuniyasu, H. Nakayama, Y. Matsushita, S. Hirono, M. Otagiri, Helix 6 of subdomain IIIA of human serum albumin is the region primarily photolabeled by ketoprofen, an arylpropionic acid NSAID containing a benzophenone moiety, Biochim. Biophys. Acta 1434 (1999) 18–30.
[28] J. Himmelfarb, E. Mcmonagle, Albumin is the major plasma protein target of oxidant stress in uremia, Kidney Int. 60 (2001) 358–363.
[29] J.P. Kehrer, Free radicals as mediators of tissue injury and disease, Crit. Rev. Toxicol. 23 (1993) 21–48.
[30] B.N. Ames, M.K. Shigenaga, T.M. Hagen, Oxidants, antioxidants, and the degenerative diseases of aging, Proc. Natl. Acad. Sci. USA 90 (1993) 7915–7922.
[31] D.D. Wayner, G. Burton, K.U. Ingold, S.J. Locke, Quantitative measurement of total, peroxyl radical-trapping antioxidant capability of human blood plasma by controlled peroxidation, FEBS Lett. 187 (1985) 33–37.
[32] B. Halliwell, J.M. Gutteridge, The antioxidants of human extracellular fluids, Arch. Biochem. Biophys. 280 (1990) 1–8.
[33] R.L. Levine, J.A. Williams, E.R. Stadtman, E. Shacter, Carbonyl assays for determination of oxidatively modified proteins, Methods Enzymol. 233 (1994) 346–363.
[34] N. Ahmed, D. Dobler, M. Dean, P.J. Thornalley, Peptide mapping identifies hotspot site of modification in human serum albumin by methylglyoxal involved in ligand binding and esterase activity, J. Biol. Chem. 280 (2005) 5724–5732.

Available online at www.sciencedirect.com
SCIENCE DIRECT®
Biochimica et Biophysica Acta 1725 (2005) 385 – 393
BIOCHIMICA ET BIOPHYSICA ACTA
BBA
http://www.elsevier.com/locate/bba

Characterization of benzodiazepine binding site on human α_1-acid glycoprotein using flunitrazepam as a photolabeling agent

Victor Tuan Giam Chuang[a,c], Motoki Hijioka[a], Masaaki Katsuki[a], Koji Nishi[a], Teppei Hara[a], Ken-ichi Kaneko[a], Megumi Ueno[a], Akihiko Kuniyasu[b], Hitoshi Nakayama[b], Masaki Otagiri[a,*]

[a]*Department of Biopharmaceutics, Graduate School of Pharmaceutical Sciences, Kumamoto University, 5-1 Oe-honmachi, Kumamoto, 862-0973, Japan*
[b]*Department of Molecular Cell Function, Graduate School of Pharmaceutical Sciences, Kumamoto University, 5-1 Oe-honmachi, Kumamoto, 862-0973, Japan*
[c]*Department of Pharmacy, Faculty of Allied Health Sciences, Universiti Kebangsaan Malaysia, Jalan Raja Muda Abdul Aziz, 50300 Kuala Lumpur, Malaysia*

Received 23 March 2005; received in revised form 20 May 2005; accepted 20 May 2005
Available online 8 June 2005

Abstract

The binding of flunitrazepam (FNZP) by human α_1-acid glycoprotein (hAGP) and the relationships between the extent of drug binding and desialylation and the genetic variants of hAGP were examined. The photolabeling specificity of [^{3}H]FNZP was confirmed by findings in which other hAGP-binding ligands inhibited the formation of covalent bonds between [^{3}H]FNZP and hAGP. The photolabeling of asialo-hAGP suggested that sialic acid does not involve in the binding of [^{3}H]FNZP. No difference in the labeling could be found between the F1*S variants and A variant. Similarly, FNZP did not show a difference in binding affinity to the two genetic variants of hAGP. Sequence analysis of the photolabeled peptide indicated a sequence corresponding to Tyr91-Arg105 of hAGP.

Keywords: Human alpha 1-acid glycoprotein; Flunitrazepam; Binding site; Topology analysis; Photoaffinity labeling

1. Introduction

Human α_1-acid glycoprotein (hAGP), an acute phase protein in blood, consists of 183 amino acid residues and five N-linked oligosaccharides, with a molecular weight of 41–43 kDa [1]. It is negatively charged due to the presence of sialic acids in its glycan chains [2]. hAGP can be produced as three main genetic variants, the A variant and the F1 and S variants, which are encoded by two different genes [3]. The proportion of each variant are approximately F1 50%, S 35% and A 15% [4]. The relative occurrence of the three main phenotypes of native hAGP composition in the population was found to be about 50% for F1+S+A, 35% for F1+A and 15% for S+A [5]. There is a difference of at least 22 amino acid residues between the F1*S and A variants while the F1 and S forms differ by only a few residues [3,6]. F1*S and A variants also differ in the number of Met residues.

hAGP's basal level is approximately 20 μmol/L, but it can vary from 5- to a 10-fold range in response to stress, infection, or the effects of neoplasm in evocation of an inflammatory response [7]. In addition, changes in the expression of genetic variants of hAGP could also occur apart from its glycosylation pattern depending on the type of inflammation [8]. The biological function of this protein is not clear, though it has been reported to have an anti-inflammatory and immunomodulating role as well as protective effects [9].

In the clinical practice, hAGP is a valuable diagnostic and prognostic tool. For example, increased hAGP levels associated with advanced tumors altered the pharmacokinetics of Imatinib (STI571), a tyrosine kinase inhibitor, in leukemia patients [10]. hAGP also appears to be an independent predictor of response and a major objective prognostic factor of survival in patients with non-small cell

Abbreviations: hAGP, Human α_1-acid glycoprotein; FNZP, Flunitrazepam; PSL, photo stimulated luminescence

* Corresponding author. Tel.: +81 86 3714150; fax: +81 96 3627690.
E-mail address: otagirim@gpo.kumamoto-u.ac.jp (M. Otagiri).

0304-4165/$ - see front matter © 2005 Elsevier B.V. All rights reserved.
doi:10.1016/j.bbagen.2005.05.021

lung cancer treated with docetaxel chemotherapy [11]. In addition, hAGP binds and transports a number of endogenous and exogenous compounds including various basic and neutral drugs influencing their pharmacokinetics and pharmacodynamics [12].

Benzodiazepines are clinically important central nervous system depressants with anxiolytic, sedative, antiepileptic and muscle relaxant therapeutic actions. The major binding protein in plasma for benzodiazepines has been identified as serum albumin. However, hAGP had been shown to bind benzodiazepines with comparable affinity by Maruyama et al. [13]. In a previous study, we have shown that diazepam was able to inhibit the photoincorporation of FNZP to hAGP but not to albumin, suggesting that certain benzodiazepines bind more readily to hAGP instead of albumin and may involve different binding mechanism [14]. During acute phase reaction, albumin synthesis is decreased while that of hAGP may increase. Thus, the pharmacokinetics of drugs that are bound by both of these two proteins may be altered [15].

Due to the clinical significance of hAGP binding of drugs, especially during acute phase reactions, the topology of its binding site has been investigated with a variety of methods including chemical modification, quantitative structure activity relationship (QSAR) methods and molecular modeling [16–18]. In a study of the binding of nine diazepines to hAGP by means of fluorescence and CD (circular dichroism) spectroscopies at our laboratory, we found that benzodiazepines have one high affinity binding site [13,19].

X-ray crystallographic analysis and nuclear magnetic resonance are the major modern direct techniques to elucidate the structures of macromolecules and their complexes at atomic resolution [20,21]. However, the application of these methods to hAGP–drug complexes is not feasible at present due to the great difficulty in the crystallization of this serum glycoprotein which comprises a mixture of variants as well as glycoforms, and also lacking of a suitable expression system that is able to produce a recombinant hAGP with correct physiologically related glycans.

Photoaffinity labeling is one of the most powerful techniques, which can be used to study a ligand binding protein [22,23]. In a recent study, we have shown that [^{3}H]FNZP (Fig. 1) was able to form covalent bond upon photoirradiation to hAGP which can be inhibited by diazepam [14]. This paper reports further attempt using [^{3}H]FNZP as a photolabeling agent to elucidate the topography of binding site amino acid sequence of hAGP and to shed light on the possible binding mechanisms.

2. Materials and methods

2.1. Materials

[^{3}H]FNZP (71 Ci/mmol) was purchased from PerkinElmer Life Sciences. hAGP (purified from cohn fraction VI) was purchased from Sigma Chemical Co. Sequencing grade modified trypsin was purchased from Promega Co. (USA). Cyanogen bromide (CNBr), dithiotreitol, trifluoroacetic acid, ammonium bicarbonate, and imidazole were purchased from Nacalai Tesque (Kyoto, Japan). 4-Vinylpyridine was purchased from Wako Pure Chemical Industries, Ltd. (Osaka, Japan). Neuraminidase, resorcinol, propranolol, lidocaine, verapamil, disopyramide, dipyridamole, testosterone, indomethacin, and salicylic acid were purchased from Sigma. *N*-glycosidase F recombinant (PNGase F) was purchased from Roche (Germany). Progesterone was from Nihon Schering. FNZP, diazepam, fludiazepam (Sumitomo Pharmaceuticals), chlorpromazine, imipramine (Mitsubishi Wellpharma), warfarin (Eisai), and phenylbutazone (Ciba-Geigy Japan) were donated by the respective companies. Acenocoumarin was a gift from Dr. Janssen from the Faculty of Pharmacy, Utrecht University, the Netherlands. All other chemicals and solvents were of analytical grade.

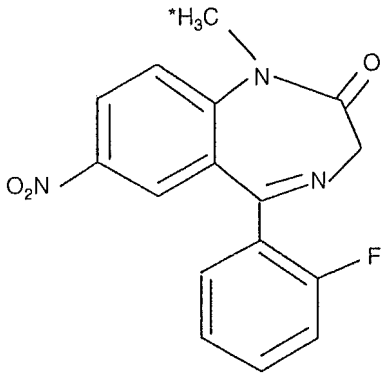

Fig. 1. Chemical structure of [^{3}H]FNZP. *: ^{3}H-labeled position.

2.2. Photoaffinity labeling of hAGP

hAGP (50 μM) was incubated with [^{3}H]FNZP (25 μM) in 100 μL of 20 mM Tris–HCl, pH 7.4, in a 1.5 mL Eppendorf tube at room temperature in the dark for 60 min. The incubation mixture was then placed on ice and irradiated for 30 min by a 100 W black light/blue lamp (Ultra-Violet Products, Inc., San Gabriel, CA, USA) at a distance of 10 cm. After irradiation, the photolabeled hAGP was precipitated by adding 1 mL of acetone, followed by centrifugation at 15 × 1000 rpm for 10 min. The pellet was washed with 1 mL of ethanol and centrifuged a second time.

2.3. Cyanogen bromide cleavage

For cyanogen bromide cleavage reactions, the pyridylethylated pellet was then dissolved in 100 μl of cyanogen bromide (CNBr) in 70% formic acid (CNBr:Met=400:1) and incubated under N_2 for 24 h in the dark at room temperature. One milliliter of milli-Q water was added at the end of the CNBr cleavage and the mixture was lyophilized.

2.4. SDS-PAGE and electroblotting

Photolabeled hAGP was analyzed on SDS-PAGE using a 10% polyacrylamide gel according to Laemmli and a sampling buffer (10 mM Tris–HCl [pH 7.6], 1% [w/v] SDS, 20 mM dithiotreitol, 4 mM ethylenediaminetetraacetic acid and 2% [w/v] sucrose) [24]. The concentration of the protein was determined by Bradford assay with bovine serum albumin as standard [25]. The gel after electrophoresis was electrophoretically transferred onto a polyvinylidene difluoride membrane in a transfer buffer (25 mM Tris, 193 mM glycine, 10% methanol) by using a semidry blotting assembly. The blotted membrane was stained with Coomassie Brilliant Blue R250, followed by drying completely in air.

2.5. Autoradiograpic analysis

For autoradiographic analysis, the dried PVDF membrane was then placed in contact with an imaging plate (BAS III, Fuji Photo film Co.) in a cassette (BAS cassette 2040) at room temperature for 48 h. The imaging plate was scanned and analyzed using a Bio-Imaging Analyzer BAS 5000 model (Fuji Photo Film Co.) and analyzed using the Fuji Film Science Lab 98 software, L Process V1.6. The incorporation of radioactivity into individual fragments was quantified by using the software Image Gauge V3.1 (Fuji Film).

2.6. Reductive pyridylethylation and deglycosylation of hAGP

After the photolabeled hAGP was precipitated by acetone, 100 μL of the buffer was added to the protein precipitate. 10 μL of 1% sodium dodecyl sulfate (SDS) and 1 M (2-mercaptoethanol) were added to this solution, before reduction were performed at 100 °C at 10 min. For deglycosylation of hAGP, 10 μL of 10% *n*-octanoyl-*N*-methyglucamide (MEGA-8), 50 μL of deionized water and 2 units of PNGase F were added to the reduction solution, and this solution was incubated for 24 h. After the addition of 1 μL of 4-vinylpyridine, the mixture was further incubated under N_2 for 30 min at room temperature in the dark and dialyzed for desalination.

2.7. Separation of hAGP Genetic Variants

The hAGP genetic variants were separated using the method of Herve et al. [26]. An iminodiacetate (IDA) Sepharose gel loaded with copper (II) ions and equilibrated in buffer 1 (20 mM sodium phosphate buffer, pH 7.0, containing 0.5 M sodium chloride) was packed into a glass column (2.0 × 30.0 cm L, Pharmacia LKB). Commercial hAGP (70 mg dissolved in 1.0 mL of buffer 1) was applied to the column at a flow rate of 1.0 mL/min. Fractions (10 mL) were collected, and their respective absorbance values were determined spectrometrically at 280 nm. As soon as the F1*S variant flowed through the column, elution buffer 2 (buffer 1 plus 20 mM imidazole) was applied to the column to remove the bound A variants. The peak fractions of each eluent were collected, concentrated on YM 10 membrane filter (Amicon, Danvers, MA), dialyzed against deionized water, and lyophilized. The purities of the isolated hAGP preparations were determined by isoelectric focusing (IEF) followed by incubation at 37 °C for 24 h with 1 unit of neuraminidase [27].

2.8. Desialylation of hAGP

hAGP was desialylated enzymatically, using the methodology described by Primozic and McNamara [27], using an immobilized neuraminidase obtained from *Clostridium perfringens*. The sialic acid content was determined by the thiobarbituric acid method. The product was dialyzed against deionized water and the dialysate was lyophilized. Approximately 95% of the sialic acid was removed, leaving an average of one sialic acid residue per protein molecule. The molecular weight of desialylated hAGP was therefore 40,000.

2.9. Determination of binding constant

Aliquots of various ratios of FNZP (5–40 μM)–hAGP (10 μM) were transferred to amicon MPS-1 micropartition system with YMT ultrafiltration membrane, centrifuged at 2000 rpm for 40 min at 25 °C. The free concentration of FNZP was determined by HPLC in a system consisting of a Hitachi 655A-11 pump and Hitachi 655A at 250 nm. A column of LichroCART 250-4, Lichrospher, RP-Select B (5 μm, 4 mm i.d. × 250 mm; Kanto Chemical) was used. The mobile phases consisted of 0.02 M KH_2PO_4 buffer (pH 2.5)–acetonitrile (6:4, v/v).

Binding parameters were determined by fitting the experimental data to the following Scatchard equation using a non-linear squares program (MULTI program) [28].

$$\frac{r}{D_f} = nK - rK$$

where n is the number of binding sites, K the binding constant and D_f the free drug concentration, with r denoting the moles of bound ligand per mole of total protein.

2.10. Tryptic digestion and purification of photolabeled hAGP peptide fragments

Tryptic digestion was done in 50 mM NH_4HCO_3 (pH 7.8). After deglycosylation, deglycosylated hAGP was incubated with trypsin for 5 h at 37 °C. The ratio of a trypsin:hAGP is 1:20 (w/w). Tryptic peptides were sepa-

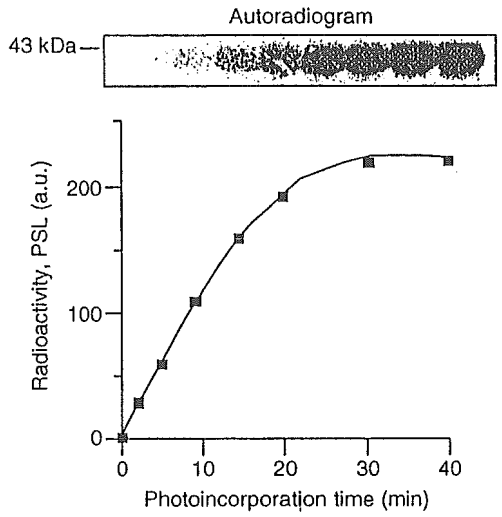

Fig. 2. Time course of [^{3}H]FNZP photoincorporation. 50 μM hAGP was incubated with 25 μM [^{3}H]FNZP for 60 min prior to photoirradiation. Aliquots of 100 μL was taken from the mixture solution at each time point as stated in the figure during irradiation until 30 min. All samples were separated with 10% SDS-PAGE and electroblotted onto a PVDF membrane for autoradiographic analysis. PSL: photo stimulated luminescence.

rated by reverse-phase C_{18} HPLC using an aqueous acetonitrile gradient in the presence of 0.1% TFA. The separated peptides fractionated every 30 s and 200 μL of each fraction was added to 2.5 mL of scintillation cocktail, and the radioactivity was determined using a LSC-500 liquid scintillation counter (Aloka, Tokyo, Japan). Then, the fraction that has the highest radioactivity was collected and was evaporated on a speedvac evaporator until the volume of the sample reached about 50 μL in the Eppendorf tube.

2.11. Capillary HPLC separation and sequencing

After evaporating, 10 μL of the sample was then injected onto the ABI 173 A MicroBlotter Capillary HPLC System, Perkin Elmer. The sample was manipulated following the manufacturer's instructions (User's Manual, 90,3836 *Rev A*, November 1995, Perkin Elmer). Meanwhile, the blotted membrane from the capillary HPLC separation was in contact with an imaging plate for 48 h prior to autoradiographic analysis. The PVDF membrane was positioned with the chromatogram of a peptide map from the ABI 173 A MicroBlotter Capillary HPLC System. Portions of the PVDF membrane were excised for sequencing on an Applied Biosystems Procise Sequencer with reference to the autoradiogram.

2.12. Statistical analysis

All data are presented as means±S.D. Statistical analysis of difference was determined by one-way ANOVA followed by the modified Fisher's least squares difference method.

3. Results

3.1. Photolabeling of [^{3}H]FNZP to hAGP

The autoradiogram in Fig. 2 shows that a band of radiolabeled protein appeared only upon the photoirradiation of hAGP with [^{3}H]FNZP in a time-dependent manner. The radioactivity band indicated covalent incorporation of [^{3}H]FNZP to hAGP via photoirradiation. The absence of a radioactive band in the sample without irradiation indicated that no covalent attachment of [^{3}H]FNZP to hAGP occurred in the dark. A 30-min exposure to light was sufficient for the covalent attachment of [^{3}H]FNZP to hAGP (Fig. 2).

3.2. Inhibitory effects of various drugs on binding of [^{3}H]FNZP to hAGP

Previous studies indicated that hAGP has one common drug binding site, which appears to be wide and flexible, comprising basic drugs, acidic drugs and steroid hormone binding regions [29]. In the photoinhibition experiment, all competitors that are known to bind hAGP, except phenylbutazone, successfully inhibited the photoincorporation of FNZP to an extent of more than 50%. In contrast, salicylic acid, which is not a binding ligand of hAGP, did not inhibit the photoincorporation (Fig. 3).

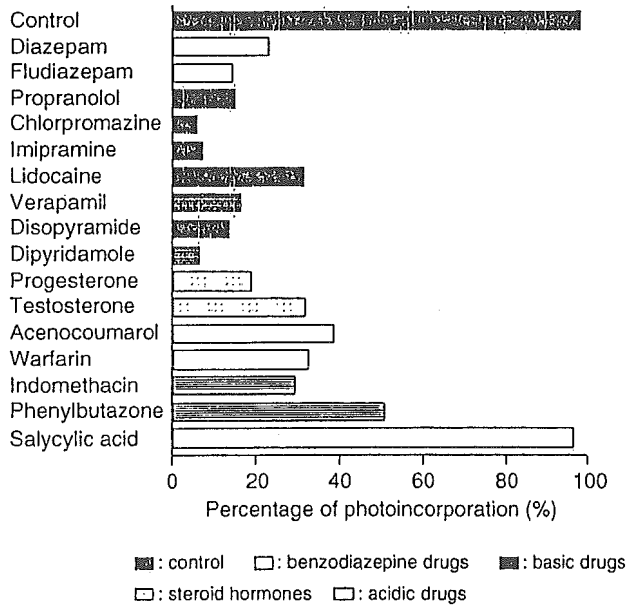

Fig. 3. Photoincorporation percentage of hAGP with [^{3}H]FNZP in the presence of various inhibitors. hAGP (50 μM) was incubated with [^{3}H]FNZP (25 μM), in the presence of competitors (250 μM) prior to photolysis. The photolabeled hAGP was cleaved with CNBr, separated with a 10% gel SDS-PAGE and electroblotted onto a PVDF membrane before being subjected to autoradiographic analysis. Radioactivity of the 34 kDa band was compared among different competitors.

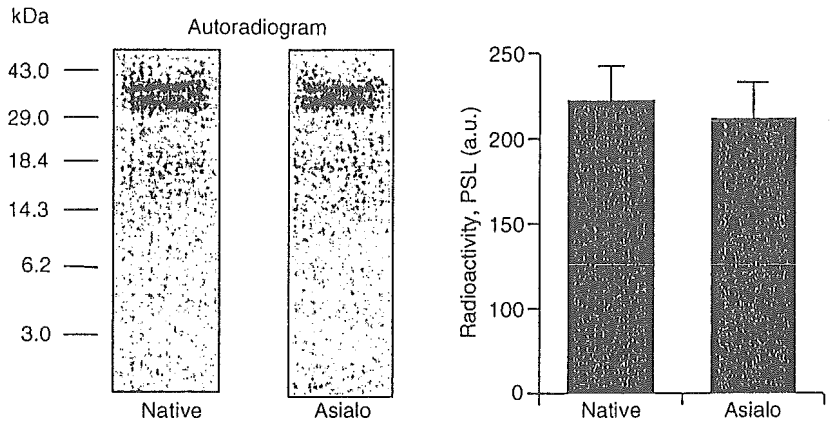

Fig. 4. Cyanogen bromide fragments of native and asialo hAGP photolabeled with [^{3}H]FNZP. 50 μM hAGP (native or asialo hAGP) was incubated with 25 μM [^{3}H]FNZP for 60 min prior to photoirradiation, and after photoirradiation, cleaved with CNBr and separated with tricine gel electrophoresis and electroblotted onto a PVDF membrane for autoradiographic analysis.

3.3. Autoradiogram of CNBr fragments of native and asialo hAGP photolabeled with [^{3}H]FNZP

hAGP possesses five N-glycan chains with sialic acids as the terminal group. The carbohydrate content of hAGP is about 45% (w/w) of molecular weight, including 14 sialic acid residues per molecule [6,30]. Sialic acid residues have been reported to influence the binding of several drugs to hAGP [31]. Nevertheless, photolabeling experimental results showed no significant difference in the extent of photoincorporation of FNZP into asialo-hAGP and native hAGP (Fig. 4). This indicated that sialic acids do not play an important role in the binding interaction of FNZP to hAGP.

3.4. Autoradiogram of CNBr fragments hAGP variants photolabeled with [^{3}H]FNZP

The A variant and the F1*S variant differ in their amino acid sequence by at least 22 residues (Fig. 5) [3,6,32]. Large differences in the binding of various drugs have been reported for the F1*S vis-a-vis the A variant [17]. The most abundant F1*S variant possesses only one Met at position 111, whereas the A variant possesses two Met at positions 111 and 156. The electrophoretic pattern of the CNBr fragment of native hAGP will thus show a band of about 34 kDa and three bands of smaller molecular weights (about 9.8, 6.0 and 3.8 kDa) (Fig 6). The peptide band of about 34 kDa corresponds to residues 1–111, and three bands of about 9.8, 6.0 and 3.8 kDa correspond to residues 112–183 and 112–156, and 157–183, respectively. Since the 34-kDa peptide of hAGP photolabeled with [^{3}H]FNZP showed the highest radioactivity, the covalent bond formation site of FNZP is located within the sequence from the N-terminus to Met111. In addition, no significant difference could be found for the extent of photoincorporation of FNZP among the two genetic variants (F1*S and A). Furthermore, there is no significant difference in the Ka values of FNZP to native hAGP, F1*S and A (Table 1, Fig. 7).

3.5. Amino acid sequence of the photolabeled tryptic peptides

The tryptic digestion of the sample was separated and simultaneously blotted onto a strip of PVDF membrane

	10	20	30	40
F1*S	QIPLCANLVP	VPITNATLDQ	ITGKWFYIAS	AFRNEEYNKS
A	QIPLCANLVP	VPITNATLDR	ITGKWFYIAS	AFRNEEYNKS
	50	60	70	80
	VQEIQATFFY	FTPNKTEDTI	FLREYQTRQD	QCLYNTTYLN
	VQEIQATFFY	FTPNKTEDTI	FLREYQTRQN	QCFYNSSYLN
	90	100	110	120
	VQRENGTISR	YVGGQEHFAH	LLILRDTKTY	MLAFDVNDEK
	VQRENGTVSR	YEGGREHVAH	NLELRDTKTL	MFGSYLDDEK
	130	140	150	160
	NWGLSVYADK	PETTKEQLGE	FYEALDCLRI	PKSDVVYTDW
	NWGLSFYADK	PETTKEQLGE	FYEALDCLCI	PRSDVMYTDW
	170	180		
	KKDKCEPLEK	QHEKERKQEE	GES	
	KKDKCEPLEK	QHEKERKQEE	GES	

Fig. 5. Amino acid sequence of hAGP variants. Differences in the amino acid sequence between the F1*S and A variant are underlined.

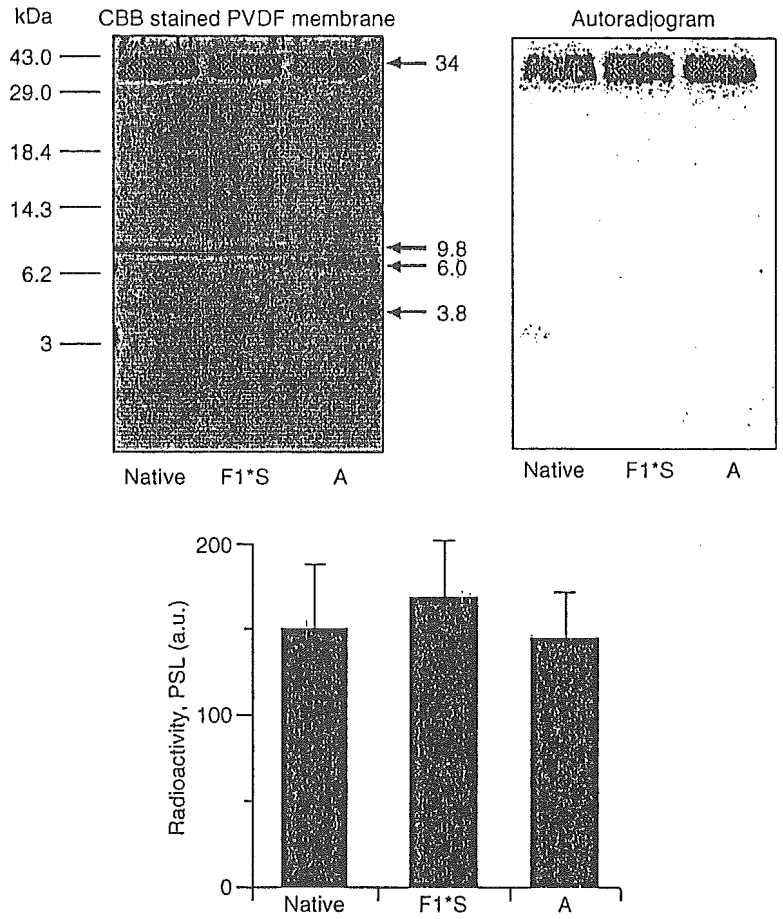

Fig. 6. Cyanogen bromide fragments of native and hAGP variants photolabeled with [^{3}H]FNZP. 50 μM hAGP (native, F1*S or A) was incubated with 25 μM [^{3}H]FNZP for 60 min prior to photoirradiation, and after photoirradiation, cleaved with CNBr and separated with tricine gel electrophoresis and electroblotted onto a PVDF membrane for autoradiographic analysis.

with an ABI 173 A MicroBlotter Capillary HPLC System. Autoradiographic analysis of the PVDF membrane indicated that the radioactive spot corresponded to the observed peak at about 40 min (Fig. 8a, b). Edman sequencing performed on the tryptic peptide of the hAGP photolabeled with [^{3}H]FNZP revealed an amino acid sequence of YVGGQEHFA (Fig. 9), corresponding to the Tyr91-Arg105 peptide sequence on F1*S variant of hAGP digested with trypsin. The YEGGREHVA sequence (91–99 in variant A) was not detected along with the YVGGQEHFA (F1*S variant) sequence, could be due to the presence of an arginine residue for variant A at position 95, thereby producing much shorter tryptic peptides, which were not eluted at a similar retention time as the peptide of F1*S variant containing the YEGGREHVA sequence. In addition, the lower abundance of variant A (15%) in the AGP sample might have contributed to the observation too [4].

Table 1
Binding parameter of FNZP to hAGP variants at pH 7.4 and 25 °C

hAGP	Ka ($\times 10^4$ M^{-1})	n
Native hAGP	2.95±1.85	1.10±0.14
F1*S	2.92±2.29	1.06±0.14
A	2.67±1.24	0.95±0.26

4. Discussion

FNZP has been successfully used as a photoaffinity labeling agent in topology analysis of the GABA receptors

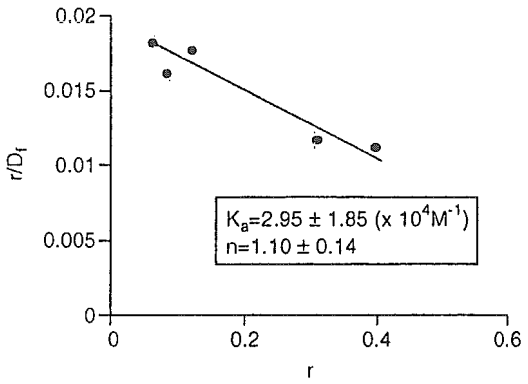

Fig. 7. Typical Scatchard plot of FNZP to hAGP. Binding experiments were performed at pH 7.4 and 25 °C.

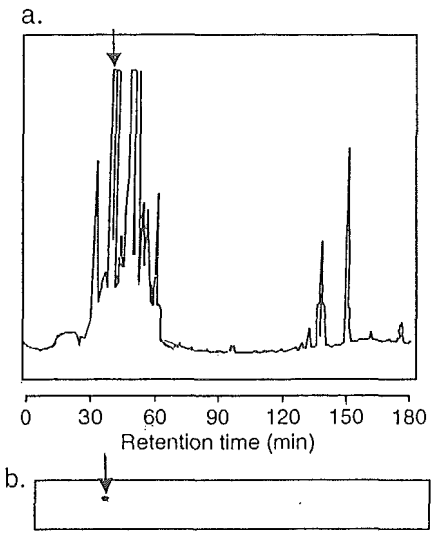

Fig. 8. Chromatogram of capillary HPLC and autoradiogram of blotted PVDF membrane. The major radioactive peptides were collected and concentrated with a speedvac evaporator. The concentrated sample from previous reversed-HPLC analysis was separated and simultaneously blotted onto a strip of PVDF membrane with an ABI 173 A MicroBlotter Capillary HPLC System. The blotted membrane from the capillary HPLC separation was in contact with an imaging plate for 48 h prior to autoradiography analysis. (a) peptides detected at UV-absorption (210 nm); (b) autoradiogram of blotted PVDF membrane.

[33,34]. In order to elucidate the binding cavity topology of hAGP, we used FNZP as a photolabeling probe. The covalent bond formation site of FNZP is located within the sequence from the N-terminus to Met111 (Fig 6). Previous studies indicated that hAGP has one common drug binding site, which appears to be wide and flexible, comprising basic drugs, acidic drugs and steroid hormone binding regions [29]. Differences in the binding of drugs to this two main genetic variants have been reported: Disopyramide, imipramine and methadone bind selectively to the A variant, whereas dipyridamole, quinidine and mifepristone bind preferentially to the F1*S variant. Progesterone, propranolol and chlorpromazine show no selectivity in binding [17]. No significant difference in the Ka values of FNZP to native hAGP, F1*S variant and A variant could be found among these three species of proteins (Table 1). In agreement with the binding experiment results, no significant difference could be found for the extent of photoincorporation of FNZP among these two species of proteins (Fig. 6). These results suggest that FNZP indiscriminately binds to F1*S and A variants. In addition, in the photoinhibition experiment, all drugs that are known to bind hAGP, except phenylbutazone, successfully inhibited the photoincorporation of FNZP to an extent of more than 50%. In contrast, salicylic acid used as a negative control which is not a binding ligand of hAGP did not inhibit the photoincorporation (Fig. 3).

hAGP possesses five N-glycan chains, which have di-, tri-, and/or tetraantennary structures, with sialic acids as the terminal group. The glycan structures show microheterogeneity under physiological conditions [35], and the partially desialylated hAGP is known to exist in plasma of patients with liver disease [36]. Sialic acid residues have been reported to influence the binding of several drugs to hAGP [31]. For example, the binding affinity of chlorpromazine was significantly decreased upon the elimination of sialic acid residues [37], whereas those of several phenothiazine neuroleptics, except chlorpromazine, decreased moderately [38]. In contrast, there are also reports that indicate the noninvolvement of sialic acid in the binding of drugs such as dicoumarol [39,40]. Our photolabeling experimental results showed no significant difference in the extent of the photoincorporation of FNZP into asialo-hAGP and native hAGP (Fig. 4). This indicated that sialic acids do not play an important role in the binding interaction of FNZP to hAGP.

Edman sequencing of the peptide photolabeled with [^{3}H]FNZP revealed an amino acid sequence of YVGG-QEHFA (Fig. 9), corresponding to the Tyr91-Arg105 peptide sequence on hAGP digested with trypsin. This is in agreement with our previous finding shown in Fig. 3. Since the His102 residue of alpha subunit of the GABA (γ-aminobutyric acid) receptor has been identified as the photolabeled site of [^{3}H]FNZP [34], we speculate that His97 and His100 of hAGP may be the amino acid residues forming a covalent bond with FNZP. Confirmation experiments are currently underway.

Maruyama et al. reported that the binding parameters (nK) of the benzodiazepine:HSA systems are slightly higher than those of the benzodiazepine:AGP systems [13]. Since benzodiazepines bind to both albumin and AGP at comparable affinity (Ka=10^4–10^5), binding to AGP in the acute phase is expected to have higher clinical significance because hAGP concentration increases 3- to 10-fold during infection, diseases with inflammatory component as well as psychiatric illness. In addition, the plasma albumin level decreases during acute phases [41]. This could significantly alter the free plasma concentrations of the ligand and contribute to its variable kinetic behavior [42].

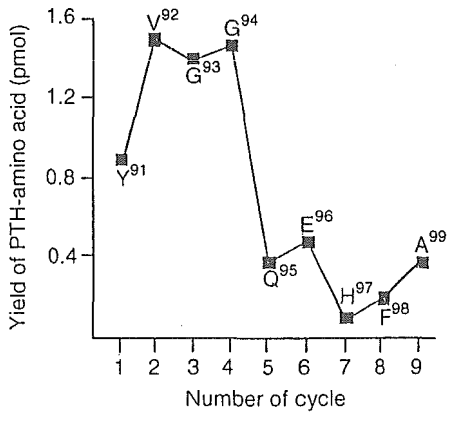

Fig. 9. N-terminal amino acid sequence analysis by the Edman degradation method. PTH: phenylthiohydantoin.

References

[1] K. Schmid, R.B. Nimberg, A. Kimura, H. Yamaguchi, J.P. Binette, The carbohydrate units of human plasma alpha1-acid glycoprotein, Biochim. Biophys. Acta 492 (1977) 291–302.

[2] T. Fournier, N. Medjoubi, D. Porquet, Alpha-1-acid glycoprotein, Biochim. Biophys. Acta 1482 (2000) 157–171.

[3] L. Dente, M.G. Pizza, A. Metspalu, R. Cortese, Structure and expression of the genes coding for human alpha 1-acid glycoprotein, EMBO J. 6 (1987) 2289–2296.

[4] F. Hervé, J.-C. Duché, J.P. Tillement, J. Testa, J. Barré, Structural aspects of alpha1-acid glycoprotein and its interaction, in: M. Otagiri, Y. Sugiyama, B. Testa, J.P. Tillement (Eds.), Proceedings of the International Symposium on Serum Albumin and Alpha1-acid Glycoprotein, Tokyo Print, Kumamoto, Japan, 2000, pp. 87–113.

[5] C.B. Eap, P. Baumann, Genetic polymorphism of human alpha-1-acid glycoprotein, in: P. Baumann, C.B. Eap, W.E. Muller, J.P. Tillement (Eds.), Alpha-1-acid Glycoprotein: Genetics, Biochemistry, Physiological Functions, and Pharmacology, Prog. Clin. Biol. Res., vol. 300, Alan R. Liss, Inc., New York, 1985, pp. 111–125.

[6] L. Dente, G. Ciliberto, R. Cortese, Structure of the human alpha 1-acid glycoprotein gene: sequence homology with other human acute phase protein genes, Nucleic Acids Res. 13 (1985) 3941–3952.

[7] D.A. Cheresh, D.H. Haynes, J.A. Distasio, Interaction of an acute phase reactant, alpha 1-acid glycoprotein (orosomucoid), with the lymphoid cell surface: a model for non-specific immune suppression, Immunology 51 (1984) 541–548.

[8] J.C. Duche, S. Urien, N. Simon, E. Malaurie, I. Monnet, J. Barre, Expression of the genetic variants of human alpha-1-acid glycoprotein in cancer, Clin. Biochem. 33 (2000) 197–202.

[9] T. Hochepied, F.G. Berger, H. Baumann, C. Libert, Alpha(1)-acid glycoprotein: an acute phase protein with inflammatory and immunomodulating properties, Cytokine Growth Factor Rev. 14 (2003) 25–34.

[10] C. Gambacorti-Passerini, M. Zucchetti, D. Russo, R. Frapolli, M. Verga, S. Bungaro, L. Tornaghi, F. Rossi, P. Pioltelli, E. Pogliani, D. Alberti, G. Corneo, M. D'Incalci, Alpha1 acid glycoprotein binds to imatinib (STI571) and substantially alters its pharmacokinetics in chronic myeloid leukemia patients, Clin. Cancer Res. 9 (2003) 625–632.

[11] R. Bruno, R. Olivares, J. Berille, P. Chaikin, N. Vivier, L. Hammershaimb, G.R. Rhodes, J.R. Rigas, Alpha-1-acid glycoprotein as an independent predictor for treatment effects and a prognostic factor of survival in patients with non-small cell lung cancer treated with docetaxel, Clin. Cancer Res. 9 (2003) 1077–1082.

[12] Z.M. Liang, K. Halifax, W.E. Lindup, D.J. Back, Elevated alpha-1-acid glycoprotein reduces the volume of distribution and systemic clearance of saquinavir, Drug Metab. Dispos. 29 (2001) 299–303.

[13] T. Maruyama, M.A. Furuie, S. Hibino, M. Otagiri, Comparative study of interaction mode of diazepines with human serum albumin and alpha 1-acid glycoprotein, J. Pharm. Sci. 81 (1992) 16–20.

[14] V.T.G. Chuang, M. Otagiri, Flunitrazepam, a 7-nitro-1,4-benzodiazepine that is unable to bind to the indole-benzodiazepine site of human serum albumin, Biochim. Biophys. Acta 1546 (2001) 337–345.

[15] I. Fitos, J. Visy, M. Simonyi, J. Hermansson, Stereoselective distribution of acenocoumarol enantiomers in human plasma: chiral chromatographic analysis of the ultrafiltrates, Chirality 5 (1993) 346–349.

[16] T. Kute, U. Westphal, Steroid–protein interactions: XXXIV. Chemical modification of alpha1-acid glycoprotein for characterization of the progesterone binding site, Biochim. Biophys. Acta 420 (1976) 195–213.

[17] F. Herve, G. Caron, J.C. Duche, P. Gaillard, N.Abd. Rahman, A. Tsantili-Kakoulidou, P.A. Carrupt, P. d'Athis, J.P. Tillement, B. Testa, Ligand specificity of the genetic variants of human alpha1-acid glycoprotein: generation of a three-dimensional quantitative structure–activity relationship model for drug binding to the A variant, Mol. Pharmacol. 54 (1998) 129–138.

[18] V. Kopecky Jr., R. Ettrich, K. Hofbauerova, V. Baumruk, Structure of human alpha1-acid glycoprotein and its high-affinity binding site, Biochem. Biophys. Res. Commun. 300 (2003) 41–46.

[19] M. Otagiri, R. Yamamichi, T. Maruyama, T. Imai, A. Suenaga, Y. Imamura, K. Kimachi, Drug binding to alpha 1-acid glycoprotein studied by circular dichroism, Pharm. Res. 6 (1989) 156–159.

[20] S. Curry, H. Mandelkow, P. Brick, N. Franks, Crystal structure of human serum albumin complexed with fatty acid reveals an asymmetric distribution of binding sites, Nat. Struct. Biol. 5 (1998) 827–835.

[21] S. Curry, P. Brick, N. Franks, Fatty acid binding to human serum albumin: new insights from crystallographic studies, Biochim. Biophys. Acta 23 (1999) 131–140.

[22] V.T.G. Chuang, A. Kuniyasu, H. Nakayama, Y. Matsushita, S. Hirono, M. Otagiri, Helix 6 of subdomain III A of human serum albumin is the region primarily photolabeled by ketoprofen, an arylpropionic acid NSAID containing a benzophenone moiety, Biochim. Biophys. Acta 1434 (1999) 18–30.

[23] M. Katsuki, V.T.G. Chuang, K. Nishi, K. Kawahara, H. Nakayama, N. Yamaotsu, S. Hirono, M. Otagiri, Use of photoaffinity labeling and site-directed mutagenesis for identification of the key residue responsible for extraordinarily high affinity binding of UCN-01 in human alpha1-acid glycoprotein, J. Biol. Chem. 280 (2005) 1384–1391.

[24] U.K. Laemmli, Cleavage of structural proteins during the assembly of the head of bacteriophage T4, Nature 227 (1970) 680–685.

[25] T. Zor, Z. Selinger, Linearization of the Bradford protein assay increases its sensitivity: theoretical and experimental studies, Anal. Biochem. 236 (1996) 302–308.

[26] F. Herve, E. Gomas, J.C. Duche, J.P. Tillement, Evidence for differences in the binding of drugs to the two main genetic variants of human alpha 1-acid glycoprotein, Br. J. Clin. Pharmacol. 36 (1993) 241–249.

[27] S. Primozic, P.J. McNamara, Effect of the sialylation state of alpha 1-acid glycoprotein on propranolol binding, J. Pharm. Sci. 74 (1985) 473–475.

[28] K. Yamaoka, Y. Tanigawara, T. Nakagawa, T. Uno, A pharmacokinetic analysis program (multi) for microcomputer, J. Pharmacobio-Dyn. 4 (1981) 879–885.

[29] T. Maruyama, M. Otagiri, A. Takadate, Characterization of drug binding sites on alpha 1-acid glycoprotein, Chem. Pharm. Bull. (Tokyo) 38 (1990) 1688–1691.

[30] M.J. Treuheit, C.E. Costello, H.B. Halsall, Analysis of the five glycosylation sites of human alpha 1-acid glycoprotein, Biochem. J. 283 (1992) 105–112.

[31] H. Shiono, A. Shibukawa, Y. Kuroda, T. Nakagawa, Effect of sialic acid residues of human alpha 1-acid glycoprotein on stereoselectivity in basic drug–protein binding, Chirality 9 (1997) 291–296.

[32] K. Schmid, in: F.W. Putman (Ed.), The Plasma Proteins, vol. 1, Academic Press, New York, 1975, pp. 183–288.

[33] R.M. McKernan, S. Farrar, I. Collins, F. Emms, A. Asuni, K. Quirk, H. Broughton, Otoaffinity labeling of the benzodiazepine binding site of alpha1beta3gamma2 gamma-aminobutyric acid A receptors with flunitrazepam identifies a subset of ligands that interact directly with His102 of the alpha subunit and predicts orientation of these within the benzodiazepine pharmacophore, Mol. Pharmacol. 54 (1998) 33–43.

[34] G.B. Smith, R.W. Olsen, Deduction of amino acid residues in the GABA(A) receptor alpha subunits photoaffinity labeled with the benzodiazepine flunitrazepam, Neuropharmacology 39 (2000) 55–64.

[35] T. Pawlowski, S.H. Mackiewicz, A. Mackiewicz, Microheterogeneity of alpha 1-acid glycoprotein in the detection of intercurrent infection in patients with rheumatoid arthritis, Arthritis Rheum. 32 (1989) 347–351.

[36] E.Y. Song, K.A. Kim, Y.D. Kim, E.Y. Lee, H.S. Lee, H.J. Kim, B.M. Ahn, Y.K. Choe, C.H. Kim, T.W. Chung, Elevation of serum asialo-alpha(1) acid glycoprotein concentration in patients with hepatic cirrhosis and hepatocellular carcinoma as measured by antibody-lectin sandwich assay, Hepatol. Res. 26 (2003) 311–317.
[37] M.L. Friedman, J.R. Wermeling, H.B. Halsall, The influence of *N*-acetylneuraminic acid on the properties of human orosomucoid, Biochem. J. 236 (1986) 149–153.
[38] T. Miyoshi, K. Sukimoto, M. Otagiri, Investigation of the interaction mode of phenothiazine neuroleptics with alpha 1-acid glycoprotein, J. Pharm. Pharmacol. 44 (1992) 28–33.
[39] M.H. Rahman, T. Miyoshi, K. Sukimoto, A. Takadate, M. Otagiri, Interaction mode of dicumarol and its derivatives with human serum albumin, alpha 1-acid glycoprotein and asialo alpha 1-acid glycoprotein, J. Pharmacobio-Dyn. 15 (1992) 7–16.
[40] T. Miyoshi, R. Yamamichi, T. Maruyama, A. Takadate, M. Otagiri, Further characterization of reversal of signs of induced cotton effects of dicumarol derivatives-alpha 1-acid glycoprotein systems by protriptyline, Biochem. Pharmacol. 43 (1992) 2161–2167.
[41] J.J. Nelson, D. Liao, A.R. Sharrett, A.R. Folsom, L.E. Chambless, E. Shahar, M. Szklo, J. Eckfeldt, G. Heiss, Serum albumin level as a predictor of incident coronary heart disease: the Atherosclerosis Risk in Communities (ARIC) study, Am. J. Epidemiol. 151 (2000) 468–477.
[42] E. Tiula, L.G. Tallgren, P.J. Neuvonen, Serum protein binding of phenytoin, diazepam and propranolol in chronic renal diseases, Int. J. Clin. Pharmacol. Ther. 25 (1987) 545–552.

FEBS Letters 579 (2005) 3596–3600 FEBS 29666

Cooperative effect of hydrophobic and electrostatic forces on alcohol-induced α-helix formation of α_1-acid glycoprotein

Koji Nishi, Yoshio Komine, Norifumi Sakai, Toru Maruyama, Masaki Otagiri*

Department of Biopharmaceutics, Graduate School of Pharmaceutical Science, Kumamoto University 5-1 Oe-honmachi, Kumamoto 862-0973, Japan

Received 11 April 2005; revised 14 May 2005; accepted 16 May 2005

Available online 8 June 2005

Edited by Maurice Montal

Abstract **α_1-Acid glycoprotein (AGP) is a serum glycoprotein that mainly binds basic drugs. Previous reports have shown that AGP converts from a β-sheet to an α-helix upon interaction with biomembranes. In the current studies, we found that alkanols, diols, and halogenols all induce this conformational change. Increased length and bulkiness of the hydrocarbon group and the presence of a halogen atom promoted this conversion, whereas the presence of a hydroxyl group inhibited it. Moreover, the effect was dependent on the hydrophobic and electrostatic properties of the alcohols. These results indicate that, in a membrane environment, hydrophobic and electrostatic factors cooperatively induce the transition of AGP from a β-sheet to an α-helix.**

Keywords: α_1-Acid glycoprotein; Alcohol; α-Helix formation; Conformational transition

1. Introduction

α_1-Acid glycoprotein (AGP), a member of the lipocalin family, is a polypeptide with two internal disulfide bonds and five carbohydrate chains that account for ~40% of its total mass (36 kDa) [1,2]. It is a major binding protein for neutral and basic ligands [3–5]. Although the three-dimensional structure and biological functions are still unknown, circular dichroism (CD) measurements [6] and molecular modeling [7] have revealed that this protein is mostly made up of β-sheets in aqueous solution.

It is widely accepted that membrane transport of a drug depends on the free drug concentration in solution. However, because this hypothesis does not fully explain the uptake mechanism for some AGP-binding drugs, a protein-mediated uptake system has been proposed [8–11]. In such a system, structural changes in the protein due to interaction with membrane surfaces decrease the drug-binding capacity. We previously reported that the interaction between AGP and model biomembranes (reverse micelles and liposomes) results in a unique conformational transition (β-sheet to α-helix) and a decrease in ligand-binding capacity [12,13]. Other studies of AGP interacting with vesicles [14] and liposomes [15] also support the conclusion that AGP interacts with the membrane in circulation.

A part of this interaction is due to the fact that the membrane potential decreases the local pH relative to the bulk solution [16]. The difference in pH has been experimentally determined to be 1.6 pH units, and the calculated value reaches 2.7 pH units [17]. Indeed, there are several reports that proteins, including other lipocalins, undergo structural and functional changes under mild acidic conditions on the membrane surface [18–21]. Also, Bychkova et al. [22] reported that cytochrome *c*, a mitochondrial protein, has a molten globule state in the presence of 40% methanol (MeOH) at pH 4.0, a condition that mimics the acidic conditions and low dielectric constant of the membrane surface environment.

There are other reports that a protein with high propensity for α-helix formation can easily convert to the α-helix form at pH 2.0 in the presence of various alcohols [23–26]. In addition, Kodicek et al. [27] reported that AGP heated in the presence of methanol (MeOH) forms a similar α-helix structure. These reports suggested that this effect was due to the hydrophobic force of alcohol and this force might induce the α-helix formation in AGP. On the other hand, the factors in such conformational transition of AGP are not elucidated.

In the present study, we used various alcohols (alkanols, diols, and halogenols) to investigate the mechanism of the α-helix formation in AGP and use of these alcohols allowed examination of how negative charge on the membrane surface and hydrophobic interaction inside the membrane affects the α-helix formation in AGP.

2. Materials and methods

2.1. Materials

AGP (Cohn Fraction VI) was purchased from Sigma Chemical Co. (St. Louis, MO, USA). All alcohols were purchased form Nacalai Tesque (Kyoto, Japan). All other chemicals and solvents were of analytical grade.

2.2. Measurement of CD spectra

CD spectra were recorded in a 1-mm path length cell with a JASCO J-720 spectropolarimeter using 10 μM AGP in 20 mM sodium acetate buffer, pH 4.0. The data were expressed as the molar residue ellipticity [*θ*] at 222 nm, which is an index of α-helix content.

*Corresponding author. Fax: +81 96 362 7690.
E-mail address: otagirim@gpo.kumamoto-u.ac.jp (M. Otagiri).

Abbreviations: The abbreviations used for the alcohols are summarized in Table 1; α_1-acid glycoprotein; CD, circular dichroism; ASA, solvent-accessible surface area; ASA (T), total ASA; rASA (H), relative ASA of hydrophobic region; rASA (N), relative ASA of negative charge region; rASA (P), relative ASA of positive charge region; HE_{50}, concentration of alcohol needed to form 50% α-helix structure

0014-5793/$30.00
doi:10.1016/j.febslet.2005.05.044